

GRAFT VERSUS HOST DISEASE

Spatiotemporal single-cell profiling reveals that invasive and tissue-resident memory donor CD8⁺ T cells drive gastrointestinal acute graft-versus-host disease

Victor Tkachev^{1*}, James Kaminski^{1,2†}, E. Lake Potter^{3†}, Scott N. Furlan^{4†}, Alison Yu¹, Daniel J. Hunt¹, Connor McGuckin¹, Hengqi Zheng⁵, Lucrezia Colonna^{4‡}, Ulrike Gerdemann¹, Judith Carlson^{5§}, Michelle Hoffman⁴, Joe Olvera¹, Chris English⁶, Audrey Baldessari⁶, Angela Panoskaltis-Mortari⁷, Benjamin Watkins⁸, Muna Qayed⁸, Yvonne Suessmuth⁸, Kayla Betz¹, Brandi Bratrude¹, Amelia Langston⁸, John T. Horan⁸, Jose Ordovas-Montanes^{2,9,10}, Alex K. Shalek^{2,11,12}, Bruce R. Blazar⁷, Mario Roederer³, Leslie S. Kean^{1*}

Organ infiltration by donor T cells is critical to the development of acute graft-versus-host disease (aGVHD) in recipients after allogeneic hematopoietic stem cell transplant (allo-HCT). However, deconvoluting the transcriptional programs of newly recruited donor T cells from those of tissue-resident T cells in aGVHD target organs remains a challenge. Here, we combined the serial intravascular staining technique with single-cell RNA sequencing to dissect the tightly connected processes by which donor T cells initially infiltrate tissues and then establish a pathogenic tissue residency program in a rhesus macaque allo-HCT model that develops aGVHD. Our results enabled creation of a spatiotemporal map of the transcriptional programs controlling donor CD8⁺ T cell infiltration into the primary aGVHD target organ, the gastrointestinal (GI) tract. We identified the large and small intestines as the only two sites demonstrating allo-specific, rather than lymphodepletion-driven, T cell infiltration. GI-infiltrating donor CD8⁺ T cells demonstrated a highly activated, cytotoxic phenotype while simultaneously developing a canonical tissue-resident memory T cell (T_{RM}) transcriptional signature driven by interleukin-15 (IL-15)/IL-21 signaling. We found expression of a cluster of genes directly associated with tissue invasiveness, including those encoding adhesion molecules (*ITGB2*), specific chemokines (*CCL3* and *CCL4L1*) and chemokine receptors (*CD74*), as well as multiple cytoskeletal proteins. This tissue invasion transcriptional signature was validated by its ability to discriminate the CD8⁺ T cell transcriptome of patients with GI aGVHD from those of GVHD-free patients. These results provide insights into the mechanisms controlling tissue occupancy of target organs by pathogenic donor CD8⁺ T_{RM} cells during aGVHD in primate transplant recipients.

INTRODUCTION

T cell infiltration into secondary lymphoid organs and nonlymphoid tissues is central to T cell function and occurs during homeostatic tissue surveillance (1, 2), as well as during T cell–driven immunopathology [including auto- (3, 4) and allo-immune disorders (5, 6)] and T cell–mediated antitumor immune attack (7, 8). One of the best-studied clinical instances of T cell infiltration occurs during

acute graft-versus-host disease (aGVHD), wherein donor T cells become activated, tissue-infiltrating, and highly cytotoxic after hematopoietic stem cell transplant (HCT) (9). During aGVHD, donor T cells first populate secondary lymphoid organs, where they undergo allo-antigen priming, and then home toward and infiltrate non-lymphoid GVHD target organs (10–12). Upon infiltration, these cells induce the immunologic and clinical manifestations of aGVHD, including widespread organ damage (13). In mouse models, it has been demonstrated that donor T cells acquire tissue-resident memory (T_{RM}) features (including expression of CD103) during aGVHD (14–16). However, central questions remain concerning how these pathogenic T_{RM} are distinguished from protective T_{RM}, how donor T_{RM} become activated and cause tissue damage, and the mechanisms controlling the act of T cell invasion into target organs before their evolution into T_{RM}. Determining the drivers of this dynamic process represents a critical unmet need, with broad relevance for allo-immunity, as well as for autoimmune diseases and immuno-oncology.

One of the major barriers to understanding the control of T cell infiltration into target tissues has been the inherent difficulty in capturing the key variable of time in this process. Time is a critical variable, given that T cells are actively homing toward and infiltrating into target organs and are concordantly evolving a highly pathogenic transcriptional program. Without understanding the time dependency of T cell infiltration, we cannot fully comprehend key drivers and their dynamics. Here, we have been able to deconvolute time as

¹Division of Pediatric Hematology/Oncology, Boston Children's Hospital, Department of Pediatric Oncology, Dana-Farber Cancer Institute, Department of Pediatrics, Harvard Medical School, Boston, MA 02115, USA. ²Broad Institute of MIT and Harvard, Cambridge, MA 02142, USA. ³Vaccine Research Center, National Institute of Allergy and Infectious Diseases, National Institutes of Health, Bethesda, MD 20858, USA. ⁴Fred Hutchinson Cancer Research Center, Department of Pediatrics, University of Washington, Seattle, WA 98109, USA. ⁵University of Washington, Seattle, WA 98195, USA. ⁶Washington National Primate Research Center, Seattle, WA 98195, USA. ⁷Division of Blood and Marrow Transplantation, Department of Pediatrics, Masonic Cancer Center, University of Minnesota, Minneapolis, MN 55454, USA. ⁸Emory University School of Medicine, Atlanta, GA 30322, USA. ⁹Division of Gastroenterology, Boston Children's Hospital and Program in Immunology, Harvard Medical School, Boston, MA 02115, USA. ¹⁰Harvard Stem Cell Institute, Cambridge, MA 02138, USA. ¹¹Institute for Medical Engineering and Science (IMES), Department of Chemistry, and Koch Institute for Integrative Cancer Research, MIT, Cambridge, MA 02142, USA. ¹²Ragon Institute of MGH, MIT and Harvard, Cambridge, MA 02139, USA.

*Corresponding author. Email: victor.tkachev@childrens.harvard.edu (V.T.); leslie.kean@childrens.harvard.edu (L.S.K.)

†These authors contributed equally to this work.

‡Present address: Juno Therapeutics, Seattle, WA 98109, USA.

§Present address: St. Jude Research Hospital, Memphis, TN 38105, USA.

a variable during T cell infiltration and tissue destruction during primate aGVHD by applying serial intravascular staining (SIVS) and pairing this with multiparameter flow cytometric and single-cell transcriptomic analyses. We performed these experiments using the non-human primate (NHP) aGVHD model (17–20) to best replicate the complex dynamics and molecular drivers of clinical tissue infiltration and disease in an out-bred immunologically experienced transplant recipient. This model takes advantage of the close functional similarity of the immune systems in NHP and humans such that insights can be most rapidly translated to the clinic. SIVS allowed us to differentially label T cells longitudinally in individual animals during the process of active tissue infiltration, to ascertain the time, tissue, and donor dependence of T cell–mediated immune pathology during aGVHD.

RESULTS

Applying SIVS to a nonhuman primate aGVHD model

We built an NHP model of allogeneic HCT (allo-HCT) and aGVHD, in which a donor graft is transplanted into major histocompatibility complex (MHC)–haploidentical recipient rhesus macaques preconditioned with myeloablative total body irradiation (17, 19). For the experiments described herein, transplant recipients received no posttransplant immunosuppression, which enabled interrogation of the natural history of aGVHD (Fig. 1A and table S1). Two control cohorts, encompassing autologous HCT (auto-HCT) recipients and untransplanted healthy controls (HCs), were also analyzed (Fig. 1A). In accordance with our previous data (17, 19), allo-HCT without immunosuppression resulted in early-onset lethal aGVHD, with skin and gastrointestinal (GI) tract–predominant clinical disease (Fig. 1, B to D), coinciding with donor T cell engraftment (Fig. 1E). Despite histopathologic evidence of lymphocytic infiltration into the liver (fig. S1A), allo-HCT recipients did not develop overt clinical signs of liver dysfunction/damage, with bilirubin, alanine transaminase, aspartate transaminase, Gamma-glutamyl transferase, and alkaline phosphatase remaining relatively stable at the time of terminal analysis (fig. S1B). Thus, lethal GI aGVHD dominated the clinical outcomes in these experiments, with transplant recipients reaching humane euthanasia end points before developing overt clinical liver disease. In contrast, auto-HCT controls survived long-term without aGVHD (Fig. 1C). aGVHD clinical activity began on ~day +5 and peaked on days +7 to 8 (Fig. 1B), similar to the kinetics of mouse alloimmune T cell trafficking to GVHD target organs (13, 15). We performed a series of *in vivo* studies on day +8 after transplant to determine the mechanisms driving tissue infiltration during severe aGVHD.

To dissect the spatiotemporal compartmentalization in aGVHD, we used a method to study T cell trafficking, known as “serial intravascular staining” [SIVS; described in the companion manuscript (21)]. SIVS takes advantage of direct intravenous injection of saturating doses of α CD45 antibodies, conjugated to different fluorescent tags, which label leukocytes in the systemic circulation at the time of injection and at different time points before analysis (6 hours and 5 min, respectively). This strategy allowed us to differentiate three spatiotemporal compartments in multiple tissues (Fig. 1F). The first compartment was identified by injecting a green fluorescent Alexa Fluor 488 (AF488)–tagged α CD45 antibody 5 min before euthanasia, which restricted α CD45-AF488 labeling to the intravascular compartment (“IVas⁺” or “compartment-1”) (Fig. 1F and fig. S2). Compartments-2 and -3 were identified using a second α CD45 antibody, conjugated with the far-red fluorescent Alexa Fluor 647 (AF647),

injected 6 hours before α CD45-AF488 injection. When far-red fluorescent α CD45-AF647–stained cells migrated out of the intravascular space into tissues, they retained their fluorescent tag and thereby could be distinguished from cells that were in the intravascular space at the time of necropsy. These cells were identified as red (CD45-AF647⁺), but not green (CD45-AF488⁻), and are referred to as “compartment-2” or “recent infiltrating” cells (Fig. 1F and fig. S2). These two fluorescently tagged cell populations could be further distinguished from a third population of cells, which remained negative for both the green and red CD45 labels. These CD45-AF647⁻CD45-AF488⁻ cells were present in the tissues before the 6-hour CD45-AF647 injection, were therefore protected from α CD45 staining, and are referred to herein as “compartment-3” or “tissue-localized” cells (Fig. 1F and fig. S2).

Using the SIVS technique, we were able to deconvolute the organ-specific spatiotemporal compartmentalization of both CD4⁺ and CD8⁺ T cells after transplant (gated as shown in fig. S2, T cell subset definitions are provided in table S2). Given the central role that CD8⁺ T cells play in aGVHD-mediated organ destruction (22, 23), we concentrated our discussion on the trafficking of these cells. Results from CD4⁺ T cells are shown in supplementary figures. We identified three different classes of organs/tissues based on their relative balance of compartment-1, -2, or -3 CD8⁺ T cells (Fig. 1G). We did not purify T cells from the skin in this study, and so we limited our discussion to visceral organs and tissues. Liver and lungs contained predominantly the intravascular, compartment-1 T cells. However, unlike lung IVas⁺ cells, liver compartment-1 CD8⁺ T cell displayed a T_{RM} phenotype (fig. S3, A and B), consistent with previous work documenting the localization of liver-resident lymphocytes within a specific intrasinusoidal niche (24, 25). During aGVHD, these liver compartment-1 CD8⁺ T cells expressed the proliferation marker Ki67 as well as high proportions of cells expressing granzyme B, suggesting an activated status (fig. S3, C and D). Bone marrow and spleen contained predominantly the recently infiltrating, compartment-2 cells (as well as a large proportion of compartment-1 cells). Lymph nodes, kidneys, small intestine (with T cells isolated from the jejunum), and large intestine contained predominantly tissue-localized compartment-3 CD8⁺ T cells (Fig. 1G). Similar organ-specific compartmentalization was observed for CD4⁺ T cells (fig. S4A). These distributions did not result in statistically significant changes between the three experimental conditions (HC, auto-HCT, and aGVHD), suggesting that spatiotemporal T cell compartmentalization may be a fundamental characteristic of organ immune structure that is not affected by either homeostatic or allo-activated T cell trafficking on the time scales studied.

Combining SIVS and measurement of donor chimerism to identify T cells infiltrating GVHD target organs

Although the compartment-3–predominant organs (lymph nodes, kidney, and GI tract) all appeared similar through SIVS, by specifically tracking donor versus host T cell identity during SIVS, we found a critical distinction between these tissues after allo-HCT. This distinction was based on the balance between donor and host T cells in these tissues (Fig. 1H), reflecting the pace of replacement of recipient T cells by donor cells after allo-HCT. These studies revealed that donor-origin compartment-3 CD8⁺ and CD4⁺ T cells predominated in the lymph nodes on day +8 (Fig. 1I and fig. S4B), consistent with rapid entry of transplanted T cells and replacement of host cells early after transplant. In contrast, a substantial fraction of host-origin T cells remained in the tissue-localized compartment-3 cells of the large intestine, small intestine, kidney, and bone marrow (Fig. 1I

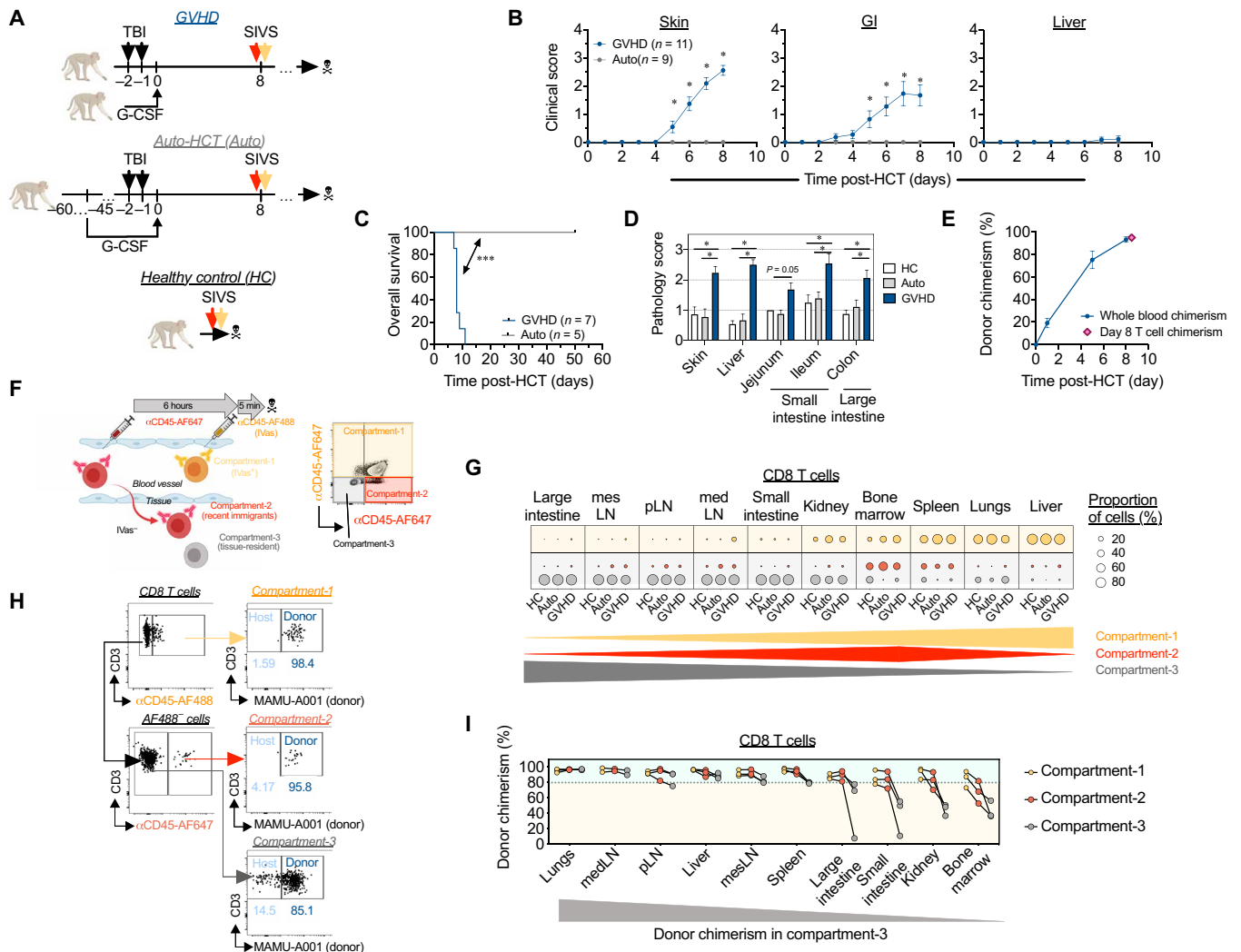


Fig. 1. Spatiotemporal compartmentalization of T cells in tissues during aGVHD. (A and B) The experimental animals received autologous or allogeneic HCT as shown in (A), and clinical aGVHD scores for skin (B, left), GI tract (B, middle), and liver (B, right) were calculated for GVHD ($n = 11$ animals) and auto-HCT ($n = 9$ animals) experimental NHP cohorts. * $P < 0.05$, using two-way analysis of variance (ANOVA) with multiple comparison Holm-Sidak posttest. (C) Overall survival of NHP recipients after allo- and auto-HCT without immunosuppression is presented. Studies with preset experimental endpoints were censored. *** $P < 0.001$ using log-rank (Mantel-Cox) test. (D) aGVHD histopathology scores were measured for indicated organs from healthy control (HC) animals or HCT recipients on day +8 after allo- or auto-HCT without immunosuppression. * $P < 0.05$, using multiple comparison Holm-Sidak test. (E) Donor chimerism in whole blood or fluorescence-activated cell sorting (FACS)-purified peripheral blood T cells from allo-HCT recipient animals was quantified by microsatellite analysis. (F) Experimental schema and representative flow cytometry plot from HC lung that illustrate the SIVS method using fluorescent α CD45 antibodies to discern cellular compartmentalization and to track cellular migration into tissues. (G) Relative distribution of CD8⁺ T cells among the intravascular compartment (compartment-1; Yellow dots), the recent infiltrating cell compartment (compartment-2; red dots), and the tissue-localized compartment (compartment-3; gray dots) in the indicated organs from HC animals ($n = 4$ animals), auto-HCT recipients (auto-HCT; $n = 4$ animals), and allo-HCT recipients (GVHD; $n = 4$ animals) on day +8 after transplant. The yellow and gray triangles and the red diamond at the bottom of the figure illustrate the pattern of the three compartments in the tissues examined. pLN, peripheral lymph nodes; medLN, mediastinal lymph nodes; mesLN, mesenteric lymph nodes. (H) Measurement of donor chimerism in the colon of an allo-HCT recipient animal, based on discordant expression of MHC-I allele MAMU-A001, in the three different compartments. (I) Donor CD8⁺ T cell chimerism in different compartments across different organs on day +8 after MAMU-A001-mismatched MHC-haploidentical allo-HCT ($n = 3$ animals). The gray triangle at the bottom of the figure illustrates the pattern of donor chimerism in the tissues examined.

and fig. S4B) during the period of active infiltration of donor T cells into these tissues. Regulatory CD4⁺ T cells (T_{REG}) represent an additional radiation-resistant population, with host T_{REG} previously demonstrated to contribute to the reconstitution of the T_{REG} pool after lethal irradiation (26, 27). To determine the relative contribution of host T_{REG} to posttransplant reconstitution, we compared conventional CD4⁺ T cell (CD4⁺ T_{CONV}) and CD4⁺ T_{REG}

donor chimerism in allo-HCT recipients after MAMU-A001-mismatched transplant. We found that, in the large intestine, a higher ratio of donor-versus-host T_{REG} were present on day +8 compared to donor-versus-host CD4⁺ T_{CONV}. This correlated with higher expression of the tissue residence marker CD69 in T_{REG} versus T_{CONV} (fig. S4, C to E). The greater donor T_{REG} chimerism in the GI tract may be due to the counter-regulatory signaling that occurs

during aGVHD (18), potentially driving these cells into the GI tract during disease.

Together, the data suggest a tenacious resident CD8⁺ T cell niche in the GI tract, kidney, and bone marrow, in which host T cells persist after transplant, even surviving lethal irradiation (28), and further link the timing of donor T cell infiltration into these tissues with the onset of clinical disease. Whereas a high proportion of host CD8⁺ T cells remained in compartment-3 in the intestines, kidney, and bone marrow, compartment-2 was dominated by donor T cells in these same tissues (with some variability observed in the bone marrow compared to other tissues; Fig. 1I and fig. S4B). This dichotomy suggests that our analysis was able to catch donor T cells in the act of organ infiltration. This is particularly relevant for donor T cells infiltrating the intestines because this infiltration was associated with lethal GI aGVHD (Fig. 1, B and C). This provided a strategy to interrogate the protein and gene expression patterns that mark these cells and to control their infiltration into aGVHD target tissues.

To rigorously distinguish pathogenic T cell infiltration during aGVHD from the physiologic T cell trafficking that occurs during homeostatic reconstitution, we used a control applying SIVS after auto-HCT. Although our studies in allo-HCT identified multiple organs undergoing T cell infiltration after transplant, homeostatic expansion occurs alongside allo-activated T cell expansion during allo-HCT, given the exposure of recipients to pretransplant lymphodepleting irradiation. Comparing the extent of tissue infiltration by compartment-2 cells in allo-HCT versus auto-HCT controls (both analyzed on day +8 after transplant) allowed us to deconvolute the role that homeostatic reconstitution played in T cell tissue infiltration. To complete this analysis, the extent of tissue migration was determined by calculating the percentage of tissue-infiltrating compartment-2 T cells compared to total extravascular (IVas⁺, compartment-2 + compartment-3) cells (representative flow cytometry from the colon shown in Fig. 2A). This analysis demonstrated that for many tissues (including peripheral and visceral lymph nodes, spleen, bone marrow, liver, lungs, and kidneys), the amount of posttransplant CD8⁺ (Fig. 2, B to D) and CD4⁺ (Fig. 2, B to D, and fig. S5, A to E) T cell migration on day +8 was not different after allo-HCT compared to post-auto-HCT conditions, suggesting that most of the T cell trafficking was in response to lymphodepletion, which abolished competition for a niche in these organs. When corrected using the auto-HCT controls, only two sites exhibited statistically significant ($P < 0.05$) differential CD8⁺ T cell infiltration during aGVHD: the large and small intestines (Fig. 2D). Only the large intestine was identified as a site of GVHD-specific CD4⁺ T cell infiltration (fig. S5E). This result is especially notable given that the GI tract has been repeatedly demonstrated in the NHP aGVHD model as key site of clinical and histopathologic disease (17, 19).

Defining the characteristics of actively infiltrating T cells

The major impact that day +8 GI T cell infiltration had on clinical aGVHD was further underscored by the positive correlation between the extent of CD8⁺ T cell migration into the large and (to a lesser extent) small intestine and the severity of aGVHD pathology in individual transplant recipients—a correlation that was not observed in any other organ (Fig. 3A). We therefore determined the prominent characteristics of donor cells infiltrating the GI tract to understand the drivers of lethal aGVHD. As shown in Fig. 3 (B to H), flow cytometry identified a number of unique attributes of intestinal tissue-infiltrating compartment-2 CD8⁺ T cells. This included

the observation that, although they were rigorously demonstrated to be extravascular and tissue infiltrating by their lack of staining by the green fluorescent IVas⁺ CD45 antibody, these intestinal compartment-2 CD8⁺ T cells did not yet coexpress the canonical T_{RM} CD69⁺CD103⁺ phenotype (Fig. 3B), consistent with their migratory phenotype. A proportion of these compartment-2 cells did, however, express CD69 (fig. S6, A and B), previously demonstrated to be up-regulated early in the process of T_{RM} differentiation, before up-regulation of CD103 expression (29).

The rapid evolution of donor CD8⁺ T cells toward the canonical T_{RM} phenotype in situ was evident, as donor CD8⁺ T cells acquired the T_{RM}-associated CD69⁺CD103⁺ dual positive phenotype during their transition from compartment-2 to compartment-3, with the highest proportion of CD69⁺CD103⁺ coexpression in residual host CD8⁺ T cells in the intestine and other nonlymphoid tissues (Fig. 3B and fig. S6, C and D), confirming their T_{RM} phenotype. Compartment-3 CD4⁺ T cells did not express CD103 (fig. S7), consistent with previous work documenting low expression of CD103 on CD4⁺ T_{RM} cells (30). These data suggest that during intestinal aGVHD, donor-derived CD8⁺ T_{RM} cells differentiate in situ from migratory precursors, likely in response to microenvironmental instructive signals [as has been demonstrated in other models (1, 31–33), including intestinal transplantation (6, 34)]. Together, these results document the rapid acquisition of a T_{RM} phenotype (within 8 days after transplant), as donor CD8⁺ T cells infiltrate and then occupy the GI tract.

Pathogenic hallmarks of actively infiltrating and T_{RM} donor CD8⁺ T cells

Flow cytometric analysis demonstrated that a large proportion of intestinal tissue-infiltrating compartment-2 CD8⁺ T cells were skewed toward a CCR7⁺CD45RA[−] effector-memory (T_{EM}) phenotype compared to both HC and auto-HCT controls, whereas other CD8⁺ T cell subpopulations (including naïve, memory stem cells, central memory, and effector memory-RA; subpopulation gating in table S2 and fig. S2) were not overrepresented in compartment-2 (Fig. 3C). These intestinal compartment-2 CD8⁺ T_{EM} cells were highly proliferative and cytotoxic during aGVHD, as measured by their increased expression of Ki67 (Fig. 3, D and E) and granzyme B (Fig. 3, F and G) compared to untransplanted and auto-HCT controls, or to host compartment-2 cells, consistent with the observed clinical pathogenicity that accompanied donor T cell tissue infiltration. Up to 44.4% of donor-derived compartment-2 CD8⁺ T cells demonstrated dual expression of granzyme B/perforin and up to 23.8% expressed granzyme B/CD107a, confirming their high cytotoxic potential (fig. S6, E and F). In the tissue-localized compartment-3, CD8⁺ T cells from healthy and auto-HCT controls, as well as the pathogenic donor T cells during aGVHD, also exhibited a prominent CD45RA[−]CCR7[−] T_{EM} phenotype (fig. S6G). However, only the compartment-3 donor cells retained high expression of Ki67 and granzyme B (along with frequent coexpression of perforin and CD107a), documenting their distinction from homeostatic compartment-3 cells and consistent with their pathogenicity (fig. S6, E, F, H, and I).

Tissue T cell chimerism is dependent on acquisition of T_{RM} characteristics by CD8⁺ donor T cells

It has previously been demonstrated that the expression of CD103 is critical for donor CD8⁺ T cell pathogenicity in the GI tract, as it enables their retention in proximity to the epithelial layer, where these cells mediate their cytotoxic functions (14, 16, 35). However,

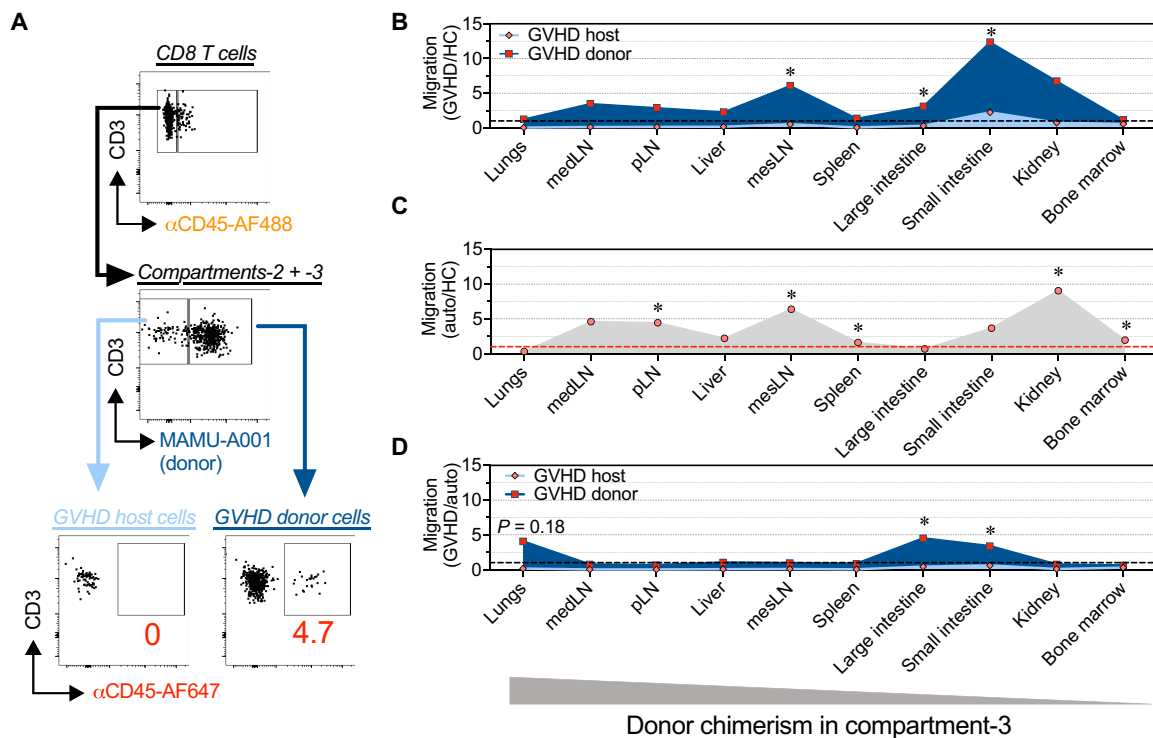


Fig. 2. Dynamics of CD8⁺ T cell trafficking into GVHD target organs after HCT in NHP. (A) Mononuclear cells were isolated from different organs from HC animals ($n = 4$) or from recipient animals on day +8 after auto-HCT ($n = 4$ animals) or MAMU-A001-mismatched allo-HCT ($n = 3$ animals). A representative gating tree depicts SIVS-based measurement of donor and host CD8⁺ T cell migration in MAMU-A001-mismatched allo-HCT transplantation. (B to D) Plots, depicting relative migration of donor and host CD8⁺ T cells from MAMU-A001-mismatched allo-HCT recipients, normalized to the migration of CD8⁺ T cells in untransplanted HC animals (B); relative migration of CD8⁺ T cells from autologous HCT recipients, normalized to the migration of CD8⁺ T cells in untransplanted HC (C); and relative migration of donor and host CD8⁺ T cells from MAMU-A001-mismatched allo-HCT recipients, normalized to the migration of CD8⁺ T cells after auto-HCT (D). pLN, peripheral lymph nodes; medLN, mediastinal lymph nodes. * $P < 0.05$ using t test with Holm-Sidak multiple comparison correction.

whether the acquisition of T_{RM} characteristics is also a foundational requirement for donor T cells to anchor in recipient tissues has previously not been a tractable question. By combining SIVS with donor chimerism measurements, we were able to directly address this issue. Our data demonstrate that the acquisition of the $CD69^+CD103^+$ phenotype was critical for establishing long-term residence in non-lymphoid tissues, as both the extent of donor CD8⁺ T cell migration into tissues and their rate of conversion into T_{RM} cells (calculations described in detail in Materials and Methods) together, but not separately, defined tissue donor CD8⁺ T cell chimerism (Fig. 3, H and I).

Determining the transcriptomes of pathogenic donor T_{RM} CD8⁺ T cells during aGVHD

SIVS allowed us to rigorously identify tissue-associated CD8⁺ T cells in HCs and after transplant. We next combined SIVS with single-cell RNA sequencing (scRNA-seq) to identify the transcriptional programs associated with the infiltration and pathogenicity of donor-derived tissue-associated CD8⁺ T cells during aGVHD. Because the data shown in Fig. 2 and fig. S3 demonstrate that the only organs experiencing allo-specific T cell infiltration at day +8 after transplant were the small and large intestines, and because the large intestine demonstrated the most robust correlation between the influx of donor CD8⁺ T cells and tissue pathology (Fig. 3A), we confined our scRNA-seq analysis to the large intestine. Before performing scRNA-seq, we flow cytometrically sorted viable, tissue-associated $CD45^+$

cells from the large intestine of HC animals ($n = 4$) and from the aGVHD cohort ($n = 4$) by gating on $IVa5^-$ (non-compartment-1) cells (table S3). Auto-HCT recipients had too few T cells in the GI tract on day 8 after transplant to reliably purify by cell sorting and thus were not included in this analysis. Where possible, donor and host cells were flow cytometrically purified based on disparate expression of MAMU-A001 (in two of the four aGVHD animals analyzed; table S1). In the two remaining allo-HCT recipients, we used computational methods to discern donor and host cells based on sex mismatch between the transplant pairs, using Y chromosome-derived transcripts (see Materials and Methods for details). Using this methodology, we successfully reconstructed transcriptomes from 21,490 single cells, followed by the identification of 14,185 T cells, based on their expression of canonical T cell genes (fig. S8). To identify 4715 CD8⁺ T cells, we used the annotation tool VISION to score each cell using a CD8⁺ versus CD4⁺ signature (36) and retained high-scoring clusters.

To systematically determine the features that differentiated pathogenic donor CD8⁺ T_{RM} in the GI tract from physiologic host or HC CD8⁺ T_{RM} , we used VISION to score a T_{RM} signature from Milner *et al.* (37) in all donor, host, and HC CD8⁺ T cells, thereby identifying the continuum of T_{RM} transcriptional programming at a single-cell level in all GI-associated CD8⁺ T cells (Fig. 4, A and B, and fig. S9A). We chose the Milner T_{RM} signature because it identifies the key genetic regulators of T_{RM} differentiation from multiple tissues regardless of

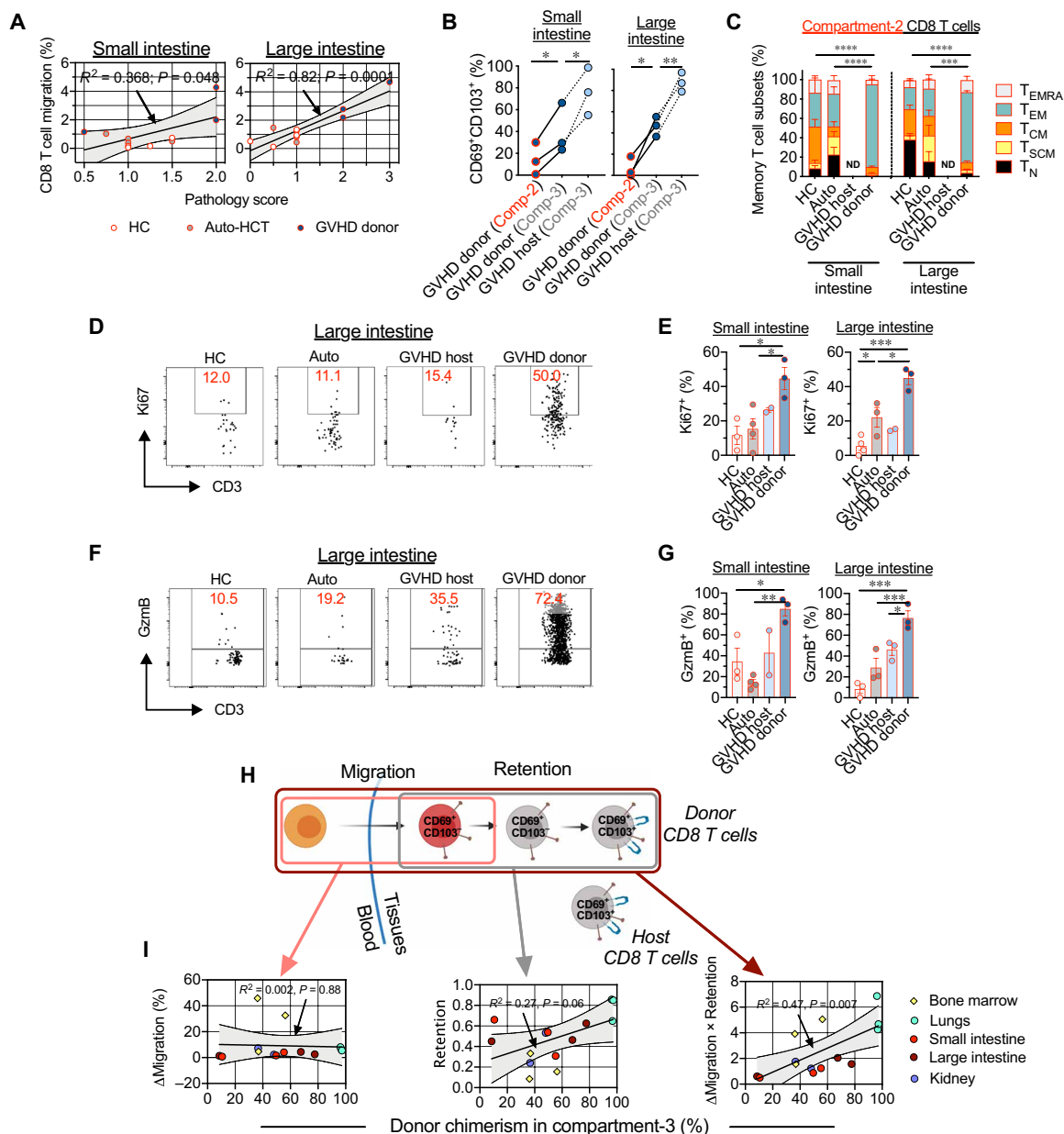


Fig. 3. Migration of donor CD8⁺ T cells to the large and small intestines correlates with the severity of tissue pathology during aGVHD in NHP. (A) Correlations between the migration of CD8⁺ T cells and GVHD histopathology scores in the small intestine (jejunum; left) and large intestine (colon; right). Lines with tinted areas indicate the 95% confidence interval (CI) using linear regression. (B) Percentage of donor or host CD69⁺CD103⁺ CD8⁺ T cells were measured within the recent infiltrating compartment (compartment-2) and the tissue-localized compartment (compartment-3). Lines connect corresponding values that were obtained from the same animal. **P* < 0.05, ***P* < 0.01 using paired *t* test. Comp-2, compartment-2; Comp-3, compartment-3. (C) Recent infiltrating (compartment-2) CD8⁺ T cells in the small and large intestines from HC animals (*n* = 4 for small intestine and *n* = 3 for large intestine), auto-HCT cohort on day +8 (Auto, *n* = 4 animals), and host (GVHD host) and donor (GVHD donor) cells after MAMU-A001-mismatched allo-HCT on day +8 (*n* = 3 animals) were stained for CCR7, CD45RA, and CD95 expression, and the distributions between memory subsets are shown. ND, no data. (D and E) Representative flow cytometry plots (D) and summary data (E) depict Ki67 expression in recent infiltrating (compartment-2) CD8⁺ T cells in the small and large intestines in different experimental cohorts. (F and G) Representative flow cytometry plots (F) and the summary data (G) depict granzyme B (GzmB) expression in recent infiltrating (compartment-2) CD8⁺ T cells in the small and large intestines in different experimental cohorts. For (E) and (G): **P* < 0.05, ***P* < 0.01, ****P* < 0.001 using one-way ANOVA with Holm-Sidak multiple comparison posttest. (H) Schematic representation of donor T cell immigration into GVHD target nonlymphoid tissues and gradual acquisition of the CD69⁺CD103⁺ T_{RM} phenotype. (I) Correlations between donor chimerism in tissue-localized CD8⁺ T cells (compartment-3) and the difference between the extent of donor and host CD8⁺ T cell migration (ΔMigration; left), extent of acquisition of the CD69⁺CD103⁺ T_{RM} phenotype in the immigrated donor CD8⁺ T cells (Retention; middle), and the difference between the extent of donor and host CD8⁺ T cell migration, adjusted to the extent of acquisition of the CD69⁺CD103⁺ T_{RM} phenotype (Migration × Retention) across different nonlymphoid organs and tissues. The lines with the tinted areas indicate the 95% CI using linear regression.

Downloaded from <https://www.science.org> at Harvard University on July 20, 2022

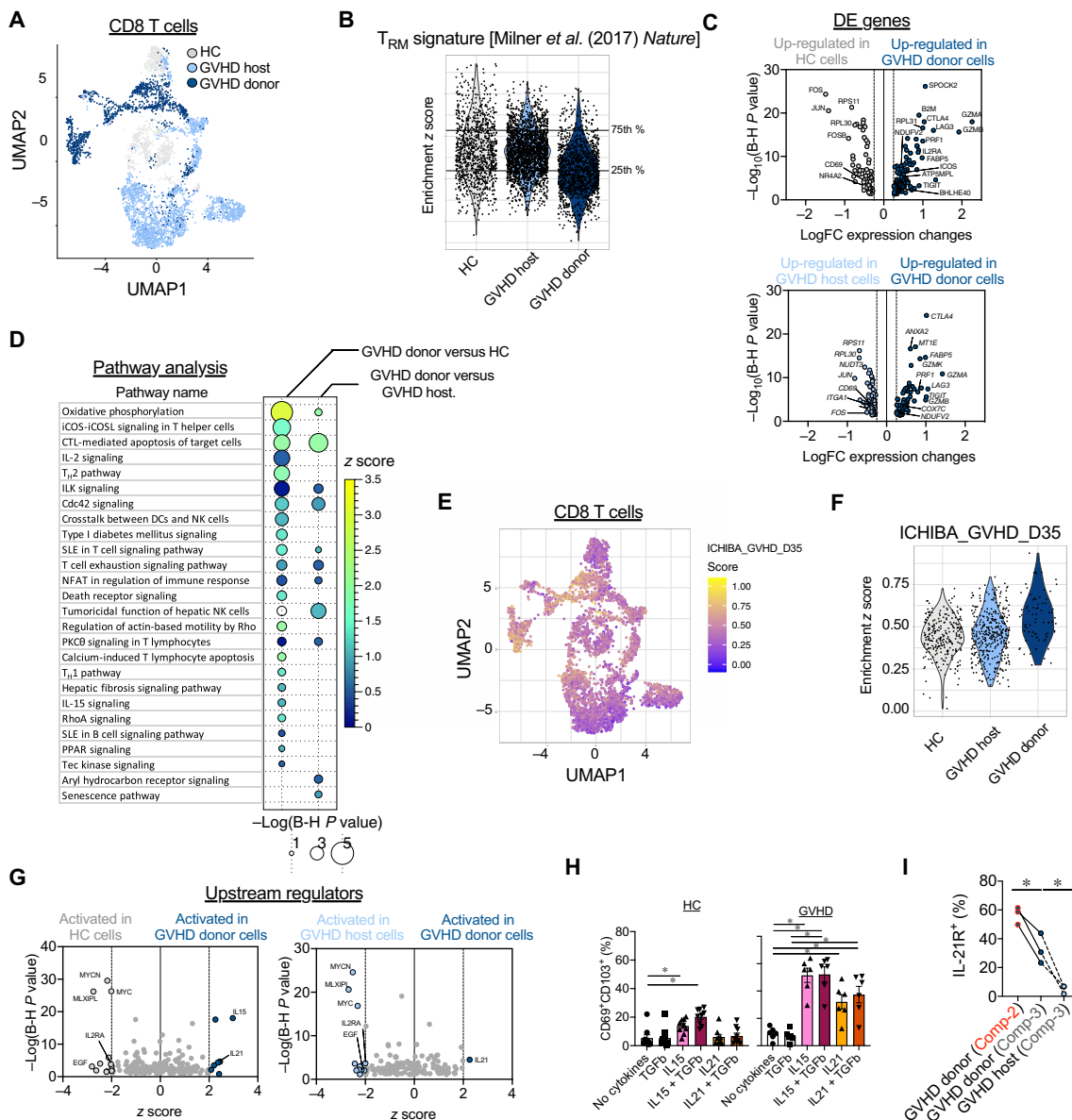


Fig. 4. Transcriptomic profile of donor-derived CD8⁺ T_{RM} cells in the large intestine during aGVHD in NHP. (A) CD8⁺ T cell census ($n = 4715$ cells), colored by experimental cohort, was clustered in uniform manifold approximation and projection (UMAP) space. **(B)** Enrichment scores for the T_{RM} signature from Milner *et al.* (37) were calculated for CD8⁺ T cells from HC animals, and host and donor CD8⁺ T cells on day +8 after allo-HCT. Horizontal lines represent the 25th and 75th percentiles for enrichment scores of the HC cohort, which were used as cutoff values to determine T_{RM}-low and T_{RM}-high cells. **(C)** Differentially expressed (DE) genes were identified between donor CD8⁺ T_{RM}-high cells and their counterparts from HC animals (HC; top) and host CD8⁺ T cells (bottom). **(D)** Pathway analysis was performed using Ingenuity Pathway Analysis on differentially expressed genes between donor CD8⁺ T_{RM}-high cells, and their counterparts from HCs and host CD8⁺ T cells. Signaling pathways with positive enrichment scores and $P < 0.05$ using t test with the Benjamini-Hochberg correction are depicted. **(E)** CD8⁺ T cell census ($n = 4715$ cells), colored by the enrichment score for the GVHD signature from Ichiba *et al.* (52), was clustered in UMAP space. **(F)** Enrichment scores for the aGVHD signature [from Ichiba *et al.* (52)] were calculated for HCs, host, and donor CD8⁺ T_{RM}-high cells. **(G)** Predicted upstream regulators were determined using Ingenuity Pathway Analysis tool performed on differentially expressed genes between donor CD8⁺ T_{RM}-high cells and their counterparts from HCs (left) and host CD8⁺ T cells (right). **(H)** Expression of IL-21R in compartment-2 and compartment-3 donor and host CD8⁺ T cells from the large intestines of MAMU-A001-mismatched allo-HCT recipients on day +8 ($n = 3$). * $P < 0.05$ using paired t test. **(I)** Spleen cells, isolated from HC animals or animals with aGVHD on day +8 after allo-HCT, were incubated with the indicated cytokines for 48 hours. Then, percentage of CD69⁺CD103⁺ CD8⁺ T cells was measured by flow cytometry. * $P < 0.05$, using one-way paired ANOVA and Holm-Sidak multiple comparison posttest.

a cell's activation status, thus providing the most accurate measure of T_{RM} transcriptional features. As shown in Fig. 4 (A and B), and in agreement with flow cytometric analysis (Fig. 3B), donor-derived GI CD8⁺ T cells had a lower mean T_{RM} score compared to either host- or HC-derived cells ($P < 0.001$ using the Wilcoxon test), con-

sistent with there being a higher proportion of actively infiltrating (rather than established T_{RM}) donor cells during GI aGVHD. Given that the Milner signature was derived from studies in mice, we also compared the NHP donor, host, and HC CD8⁺ T cells to two human-derived GI tract-specific tissue-resident T cell signatures

(Zhang_CD8_C05_CD6 and Zhang_CD8_C06_CD160) (38), which confirmed the higher T_{RM} differentiation status of large intestine host and HC $CD8^+$ T cells compared to donor $CD8^+$ T cells (fig. S9). The murine Milner signature was highly correlated with both of the human-derived intestinal T_{RM} cell signatures (fig. S9B). A third human-derived, but not GI-specific, T_{RM} signature, identified by Kumar *et al.* (39), also showed significant correlation with the Milner T_{RM} signature ($P < 0.0001$), but this non-GI-derived signature did not discriminate intestinal donor $CD8^+$ T cells from residual host $CD8^+$ T cells and $CD8^+$ T cells from HC large intestines (fig. S9, C to E). This observation may have been expected, given previous work that has demonstrated that the transcriptomic profiles of T_{RM} cells display considerable interorgan variation (40).

To further determine what differentiated pathogenic donor $CD8^+$ T cells from both host and HC $CD8^+$ T_{RM} , we first defined a T_{RM} -high cutoff score by identifying the upper T_{RM} score quartile from HC $CD8^+$ T cells (Fig. 4B) and then applied this score cutoff to both the donor and host $CD8^+$ T cells to identify T_{RM} -high subpopulations in each. This allowed us to probe the transcriptional differentiators between pathogenic donor T_{RM} -high cells and both host and HC T_{RM} controls through differential expression (DE) calculations, followed by pathway enrichment analysis and classification of upstream regulators. This pipeline distinguished the following features of pathogenic $CD8^+$ T_{RM} cells: They develop rapidly (within 8 days) after allo-HCT, and they consist of pathogenic donor cells that simultaneously enact T_{RM} transcriptional programming in addition to up-regulation of key T cell activation programs. These programs include up-regulation of specific cellular metabolic pathways [including oxidative phosphorylation and mitochondrial respiration, which have been demonstrated to be central to both T_{RM} development (41–43) and aGVHD pathogenesis (44, 45)], costimulatory signaling pathways [including aGVHD-promoting ICOS (46, 47), interleukin-2 (IL-2) (48, 49), and OX40 (20, 50) signaling pathways], and cytotoxicity pathways (51) compared to their physiologic counterparts (Fig. 4, C and D, and tables S4 and S5). We also identified a higher enrichment score for the aGVHD pathogenicity signature adopted from Ichiba *et al.* (52) in donor T_{RM} -high cells in comparison with host and HC T_{RM} -high cells (Fig. 4, E and F), further substantiating the pathogenicity of the donor T_{RM} . Our analysis of the upstream regulators that control the activation pathways in donor T_{RM} -high $CD8^+$ T cells revealed involvement of IL-15 and IL-21 cytokine signaling (Fig. 4G and table S6), suggestive of a central role for these cytokines in T_{RM} differentiation (particularly during lymphopenic conditions) (29, 53), as well as their pathogenic role during aGVHD (54–58). We further confirmed that both IL-15 and IL-21 could induce maturation toward a $CD69^+CD103^+$ T_{RM} phenotype in NHP splenocytes *in vitro*. We found that IL-15-induced T_{RM} differentiation in splenocytes isolated both from HC animals and from those with aGVHD, whereas IL-21 promoted T_{RM} differentiation only in aGVHD-derived cells (Fig. 4H). Given our observation of the specificity of IL-21 in the differentiation of $CD8^+$ T_{RM} during aGVHD, we further investigated this biological pathway. IL-21R was expressed on both compartment-2 and compartment-3 donor $CD8^+$ T cells in the large intestine during aGVHD with higher expression on the surface of recently infiltrating compartment-2 cells. In contrast, expression of IL-21R on residual host cells was low (Fig. 4I). Both IL-21R⁺ and IL-21R⁻ donor $CD8^+$ T cells in compartments-2 and -3 demonstrated similar expression of Ki67, perforin, and granzyme B, suggesting that, as previously reported in mice (54, 58), expression

of IL-21R does not differentiate between proliferating/cytotoxic and more quiescent cells. We also measured the expression of *IL-21* itself and found a proportion of donor cells in the large intestine expressing this gene (8.69%) after allo-HCT, thus providing a local source of this cytokine during GI aGVHD (fig. S10, D to F). Together, these data identify multiple transcriptional pathways and upstream regulators that are strongly associated with aGVHD-mediated tissue destruction, providing the first direct link between T_{RM} differentiation and donor T cell pathogenesis in primate aGVHD.

Identifying transcriptional control of actively infiltrating donor $CD8^+$ T cells

In addition to identifying the drivers of pathogenic $CD8^+$ T_{RM} , this study also provided an opportunity to interrogate the transcriptional hallmarks of actively tissue-infiltrating pathogenic $CD8^+$ T cells at unprecedented specificity. To accomplish this, based on the SIVS results (Fig. 3B) that demonstrated that compartment-2 actively infiltrating cells display a migratory, rather than T_{RM} -like, phenotype, we first identified a T_{RM} -low cutoff score (by identifying the lower Milner T_{RM} score quartile from HC $CD8^+$ T cells; Fig. 4C) and then applied this score cutoff to both donor and host $CD8^+$ T cells. This allowed us to isolate donor cells that were tissue associated, given that they were first sorted as non-intravascular (compartment-1-negative) before scRNA-seq and simultaneously did not yet display features of T_{RM} . We then defined the transcriptional differentiators between pathogenic donor T_{RM} -low cells and both host and HC T_{RM} -low controls by applying DE calculations (Fig. 5A and tables S7 to S9). Similar to their donor T_{RM} -high counterparts, donor $CD8^+$ T_{RM} -low cells demonstrated high enrichment scores for the aGVHD pathogenicity signature from Ichiba *et al.* (52) (fig. S10G). In agreement with flow cytometric analysis (Fig. 3, F and G, and fig. S6, E and F), transcriptome analysis demonstrated that these cells co-expressed genes encoding multiple cytotoxic mediators (fig. S10H) also consistent with their pathogenic status. A direct comparison of donor $CD8^+$ T_{RM} -low cells with their T_{RM} -high counterparts revealed that although the T_{RM} -low cells had similar expression of the cytotoxicity-related transcripts *GZMA*, *GZMB*, and *PRF1*, they demonstrated lower expression of the genes encoding *TNFRSF1B* (59), *ID2* (60), *IFNG* (61), and *RGS1* (62) (fig. S10I and table S10), which have been demonstrated to play major roles in the pathogenicity of both GI GVHD and T cell-driven colitis. Moreover, and consistent with the role for IL-21 in T_{RM} differentiation described above (Fig. 4H), our analysis of predicted upstream regulators of T_{RM} -high versus T_{RM} -low $CD8^+$ T cells confirmed activation of IL-21 signaling in T_{RM} -high > T_{RM} -low (table S11). Together, these data suggest that, whereas compartment-2 and compartment-3 $CD8^+$ T cells both display pathogenic characteristics, compartment-3 cells express additional genes associated with auto- and allo-immunity, likely enabling them to perpetuate intestinal inflammation during GI GVHD.

Last, we focused on the T_{RM} -low-specific transcriptome by identifying those differentially expressed genes that were unique to the T_{RM} -low donor versus control comparisons (and not identified in the T_{RM} -high versus control comparisons). This analysis distinguished 53 transcripts (46 up-regulated genes and 7 down-regulated genes) that were specifically dysregulated in donor $CD8^+$ T_{RM} -low cells, as well as their associated pathways and upstream regulators (Fig. 5, B to D, and tables S12 to S14). Regulatory network analysis again identified IL-15, as well as type I and type II interferons (and their corresponding signals) as key upstream regulators controlling

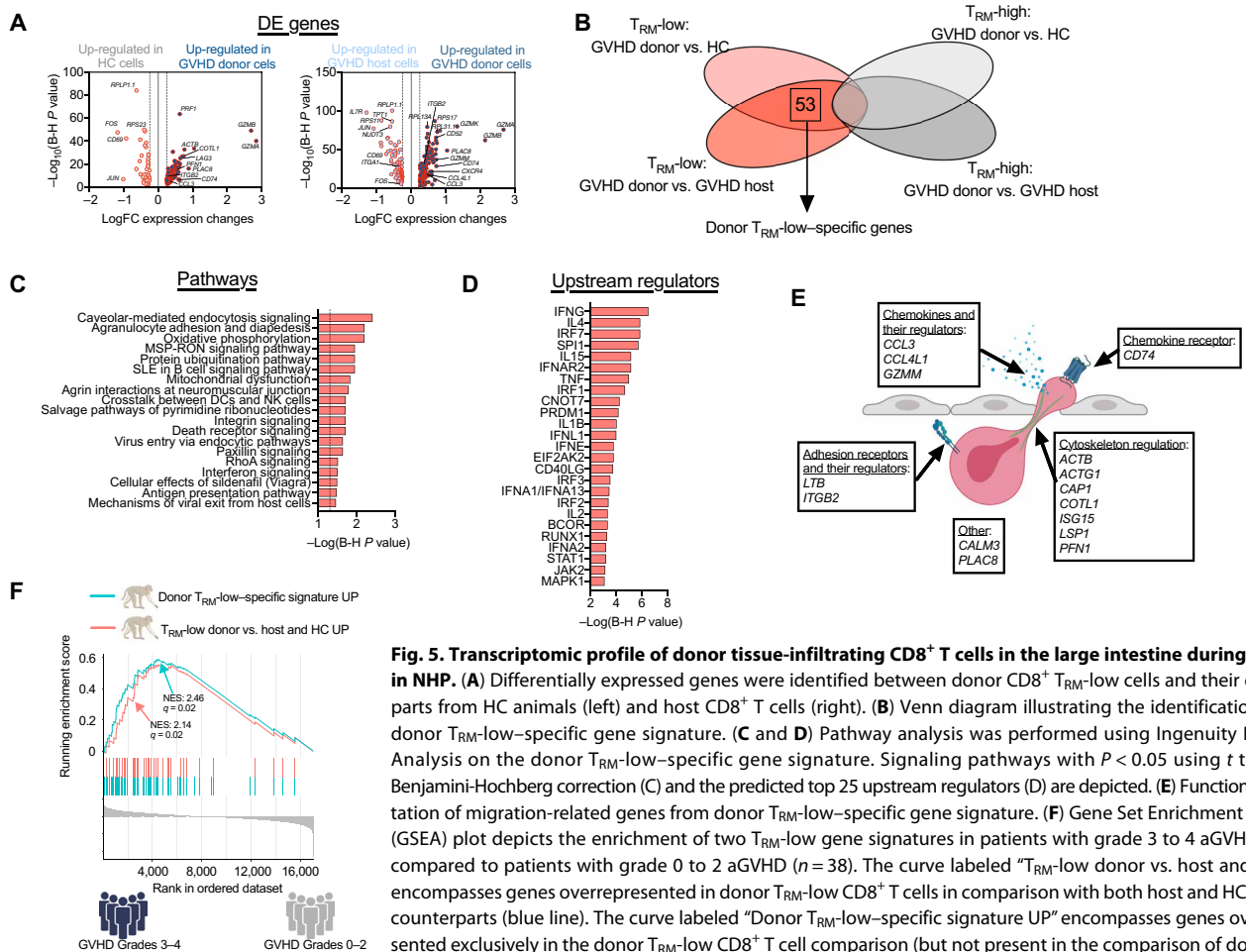


Fig. 5. Transcriptomic profile of donor tissue-infiltrating CD8⁺ T cells in the large intestine during aGVHD in NHP. (A) Differentially expressed genes were identified between donor CD8⁺ T_{RM-low} cells and their counterparts from HC animals (left) and host CD8⁺ T cells (right). (B) Venn diagram illustrating the identification of the donor T_{RM-low}-specific gene signature. (C and D) Pathway analysis was performed using Ingenuity Pathway Analysis on the donor T_{RM-low}-specific gene signature. Signaling pathways with *P* < 0.05 using *t* test with Benjamini-Hochberg correction (C) and the predicted top 25 upstream regulators (D) are depicted. (E) Functional annotation of migration-related genes from donor T_{RM-low}-specific gene signature. (F) Gene Set Enrichment Analysis (GSEA) plot depicts the enrichment of two T_{RM-low} gene signatures in patients with grade 3 to 4 aGVHD (*n* = 4) compared to patients with grade 0 to 2 aGVHD (*n* = 38). The curve labeled “T_{RM-low} donor vs. host and HC UP” encompasses genes overrepresented in donor T_{RM-low} CD8⁺ T cells in comparison with both host and HC T_{RM-low} counterparts (blue line). The curve labeled “Donor T_{RM-low}-specific signature UP” encompasses genes overrepresented exclusively in the donor T_{RM-low} CD8⁺ T cell comparison (but not present in the comparison of donor T_{RM-high} CD8⁺ T cells versus both host and HC T_{RM-high} counterparts) (red line). NES, normalized enrichment score.

the transcriptional programming of these donor tissue-infiltrating T cells (Fig. 5D and table S14). Pertinent to the goal of defining the drivers of T cell infiltration, we identified a subset of genes that have been shown to be critical for cellular adhesion, migration, and tissue infiltration in other clinical scenarios. These included chemokines, as well as regulators of their secretion and receptors [*CCL3* (63), *CCL4L1* (64), *GZMM* (65), and *CD74* (66)], surface adhesion receptors and regulators of their expression [*LTB* (67) and *ITGB2* (68)], and cytoskeleton components and regulators [*ACTB* (69), *ACTG1* (69), *CAP1* (70), *COTL1* (71), *ISG15* (72), *LSP1* (73), and *PFN1* (74)] (Fig. 5E). These data thus provide the first transcriptional map of this unique subpopulation of actively infiltrating donor CD8⁺ T cells, nominating a previously unidentified class of molecules that enable pathologic CD8⁺ T cell tissue invasion during GVHD.

Validating the clinical relevance of the NHP tissue infiltration transcriptional signature

To validate that the genes and pathways identified through the NHP experiments were relevant to human disease, we compared our NHP transcriptional signatures to a CD8⁺ T cell signature generated from patients with aGVHD. The human aGVHD signature was constructed from peripheral blood CD8⁺ T cells that were sorted on days +21 and +28 after transplant from 42 patients receiving an unrelated-donor HCT and standard calcineurin inhibitor/methotrexate

aGVHD prophylaxis (table S15). Twenty-eight of these patients developed grade 2 to 4 aGVHD (with 27 of 28 having either upper or lower GI disease). All patients with grade 3 to 4 aGVHD demonstrated lower GI disease (table S15). The resulting transcriptomes were dichotomized between patients who developed severe grade 3 to 4 aGVHD versus those with grade 0 to 2 aGVHD (Fig. 5F) or those with moderate-severe grade 2 to 4 aGVHD versus those with grade 0 to 1 aGVHD (fig. S10L). These analyses demonstrated significant overlap (*q* = 0.02) between the migratory donor CD8⁺ T_{RM-low} signatures and the human CD8⁺ T cell aGVHD signature (Fig. 5F, fig. S10L, and table S16). These results provide strong evidence for the relevance of the NHP data to human aGVHD, and they demonstrate the ability to probe the peripheral blood for signatures relevant to the migrating pathogenic cells that ultimately infiltrate the GI tract during clinical aGVHD. Thus, whereas the peripheral blood did not contain the complete pathologic signature derived from GI tract infiltrating T cells (table S16), the peripheral blood signature complemented the organ-specific results, which successfully dichotomized patients with moderate-to-severe clinical disease.

DISCUSSION

Here, the application of intravascular staining (75) plus scRNA-seq to NHP aGVHD has enabled the interrogation of tissue-localized

Downloaded from https://www.science.org at Harvard University on July 20, 2022

T cell immunity at an unprecedented depth of detail in an outbred, pathogen-exposed, immunologically experienced system. By applying serial infusions of differentially labeled anti-CD45 antibodies [“SIVS”; (21)], we have been able to include time as a variable in our analysis, facilitating the detection of three spatiotemporally defined T cell compartments: (i) T cells that were intravascular at the time of analysis, (ii) T cells that were intravascular 6 hours before analysis and subsequently infiltrated into target tissues, and (iii) T cells that were tissue associated for at least 6 hours before analysis and did not acquire either of the two CD45 labels. By overlaying our ability to distinguish donor versus host cells after allo-HCT onto these three compartments, we have developed a highly sensitive and specific paradigm to identify pathogenic donor CD8⁺ T cells, either in the act of organ infiltration or in the act of tissue destruction during GI aGVHD.

Our observations provide strong support for the rapid evolution of a pathogenic T_{RM} transcriptional program in donor CD8⁺ T cells after allo-HCT, representing a notable counterpart to recent observations documenting the longevity of donor-origin T_{RM} in transplanted lung and intestinal allografts (5, 6, 34). Our results demonstrate that, within 8 days after allo-HCT, donor T cells infiltrate target organs and rapidly exhibit protein and transcriptional T_{RM} hallmarks. However, despite clear expression of a T_{RM} program, when compared to either host or HC GI tract CD8⁺ T cells, the donor CD8⁺ T_{RM} are clearly not homeostatic. They up-regulate multiple transcriptional networks driving T cell activation, including evidence of both metabolic reprogramming toward mitochondrial respiration and massively up-regulated cytotoxicity pathways. Our results also identify IL-15 and IL-21 as key upstream regulators, which together coordinate the transcriptional programming responsible for the pathogenic donor CD8⁺ T_{RM} differentiation. These two cytokines have been shown to drive aGVHD in mouse models (54–57), and IL-15 signaling is required for CD8⁺ T_{RM} generation in multiple barrier tissues (29, 76). Compared to IL-15, the role of IL-21 in the generation of T_{RM} cells is far less established (53), and in this study, we provide evidence that IL-21 can drive T_{RM} differentiation from circulatory precursors during aGVHD, but not under homeostatic conditions. The demonstration of redundant T cell activation programs may provide an explanation for the well-documented difficulty of reversing ongoing clinical aGVHD: Pathogenic GI tract T_{RM} are not only physically sequestered from therapeutic agents (77, 78) but also potentially protected from monomorphic treatment approaches, given the nonoverlapping pathways that they activate.

This study also enabled the identification of the transcriptional network controlling donor CD8⁺ T cells “caught in the act” of tissue infiltration. These rare cells have previously been intractable to detailed examination because of their small numbers and their fleeting nature. Through the combination of SIVS and scRNA-seq, we were able to identify and deeply interrogate this critical cell population. By enabling flow sorting of GI tract T cells that were compartment-1 (iVas)-negative, SIVS allowed us to rigorously exclude intravascular cells from our analysis. Although compartment-2 cells were too rare in the GI tract for sorting, the fact that these cells were rigorously demonstrated to be non-T_{RM} by flow cytometry allowed us to transcriptionally identify them by their T_{RM}-low signature. Transcriptional analysis subsequently identified central features of these actively infiltrating cells. Although these include several “usual suspects” in aGVHD, comprising costimulatory/coinhibitory pathways (79), the immunoproteasome (80), and several targetable metabolic pathways (44, 45, 81), one of the most important findings was the transcrip-

tional program of adhesion/extravasation/migration that these actively infiltrating cells initiated. These represent distinct pathways compared to donor CD8⁺ T cells that had already enacted T_{RM} programming, as well as from both host and HC compartment-2 cells. The identification of tissue infiltration-associated gene networks may have relevance to other immune phenomena: These include solid organ transplant rejection and autoimmune diseases, which both require infiltration and long-term tissue persistence of pathogenic cells (82). In addition, the discovery of a CD8⁺ T cell infiltration gene network may be used to improve the ability of antitumor T cells to more successfully infiltrate their targets and survive in the tumor microenvironment, given the recently found mechanistic connections between tumor-infiltrating lymphocytes and T_{RM} biology (7, 8).

This study has the following limitations: First, we studied the nonprophylaxed “natural history” of aGVHD, and mechanisms of infiltration and pathogenic T cell residency may be altered by immunoprophylaxis. Second, this study was limited to two anti-CD45 infusions, 6 hours apart, thus constraining our ability to discriminate shorter- versus longer-lived tissue-resident cells. Additional CD45-antibody infusions will enable more precise dissection of the pace/character of pathogenic tissue residency. Last, the scRNA-seq experiments focused only on the GI tract. Mechanisms controlling aGVHD are expected to be at least partially organ-specific; thus, further work with other target tissues will add important insights.

In summary, by combining SIVS with scRNA-seq, we have interrogated pathogenic donor CD8⁺ T cells in the act of infiltrating and causing tissue destruction during GI aGVHD. Our results document a transcriptional network defining T cell infiltration during this disease and validate the clinical relevance of this network. They nominate a previously unidentified class of targets by which to control the act of T cell infiltration, which constitutes a necessary prelude to T cell-mediated organ damage.

MATERIALS AND METHODS

Study design

This was a prospective study in rhesus macaques designed to determine the biological role of T cell migration and to identify the molecular signature of pathogenic tissue-infiltrating T cells in aGVHD-induced tissue immunopathology. Several cohorts of transplant recipients (assigned in an unblinded, nonrandomized manner) were studied: (i) autologous transplants (abbreviated as “auto-HCT,” $n = 9$ for clinical analysis and $n = 4$ for immunological analysis), (ii) allogeneic transplants with no GVHD prophylaxis (abbreviated as “allo-HCT” and “aGVHD,” $n = 11$ for clinical analysis and $n = 4$ for immunological analysis, including three MAMU-A001-mismatched transplantations), and (iii) a control cohort of healthy, immunologically naïve macaques (abbreviated as “HC,” $n = 4$ for immunological analysis). Auto- and allo-HCT recipients used for SIVS experiments were euthanized at a predetermined experimental end point on day +8 and were censored from survival analysis. Animal demographic parameters, transplant characteristics, and doses of α CD45 antibodies administered in vivo are shown in table S1. Sample size calculations were not performed for the present study, given existing data from multiple previous transplant cohorts published by our group (17–20), documenting the substantial differences in median GVHD-free and overall survival after MHC-haploidentical allo-HCT versus autologous transplantation in NHP. Blinding was performed on all pathologic analysis and on the initial analysis of

flow cytometry data, as well as on transcriptomic sample handling and data processing.

NHP ethics statement

This study was conducted in strict accordance with (USDA) United States Department of Agriculture regulations and the recommendations in the *Guide for the Care and Use of Laboratory Animals* of the National Institutes of Health. It was approved by the Biomere Inc. and University of Washington Institutional Animal Care and Use Committees.

Human studies ethics statement

The patients described in this study were enrolled in clinical trial #NCT01743131 that was conducted according to the principles set forth in the Declaration of Helsinki and that was approved by participating center institutional review boards. Written informed consent was received from all participants.

HCT in NHP

We used our previously described strategy for HCT in rhesus macaques (17–19), described in detail in Supplementary Materials and Methods.

α CD45 infusions

Purified α CD45 (clone MB4-6D6) was purchased from Miltenyi Biosciences. Antibodies were conjugated in M.R.'s laboratory to Alexa Fluor dyes. Conjugated antibodies were diluted in sterile normal saline solution, and 5 ml was slowly infused over 5 min to animals via a central catheter placed in the femoral vein (auto-HCT and allo-HCT cohorts) or to sedated animals via a peripheral catheter placed in saphenous vein (HC cohort). To track lymphocyte migration, α CD45 antibodies conjugated with Alexa Fluor 647 (α CD45-AF647) were administered 6 hours before euthanasia/tissue collection at a dose of 30 μ g/kg. To discriminate tissue-residing cells from cells remaining in the vasculature, α CD45 antibodies, conjugated with Alexa Fluor 488 (α CD45-AF488), were administered 5 min before euthanasia/tissue collection at a dose of 30 or 60 μ g/kg (Fig. 1, fig. S2, and table S1). Blood samples were drawn from the catheter before and 5 min after each α CD45 antibody injection to ensure that all blood leukocytes were uniformly labeled with the injected antibodies.

Necropsy and tissue processing

Tissues from euthanized animals were processed after perfusion with phosphate-buffered saline using enzymatic digestion and mechanic separation as described in Supplementary Materials and Methods.

Immune analysis

Blinding was performed on all pathologic analysis. Flow cytometry data were collected using the BD FACS LSRFortessa and analyzed using FlowJo 10 in an unblinded manner. The gating strategy and the assessment of cellular migration using intravascular α CD45 labeling are described in fig. S2, table S2, and Supplementary Materials and Methods.

Transcriptomic analysis

Single-cell libraries from sorted samples were generated using the 10 \times Chromium 3' platform and then sequenced using NovaSeq S2 (Illumina). scRNA-seq reads were aligned to a transcriptome based on the Mmul 10 *Macaca mulatta* reference genome with Ensembl's (v98) annotations, and the analysis was performed in an unblinded

manner using Seurat v3.1, VISION, clusterProfiler, and Ingenuity Pathway Analysis (IPA) as described in Supplementary Materials and Methods. Bulk RNA-seq from human samples was trimmed using Trimmomatic v.39 (83) and aligned with kallisto v.0.46.1 (84). Analysis was performed using DESeq2 (85) and clusterProfiler (86).

Statistical analysis

Both paired and unpaired Student's *t* tests were used for comparing two groups, where appropriate. One-way analysis of variance (ANOVA) with Holm-Sidak multiple comparison posttest or two-way ANOVA analysis with Holm-Sidak multiple comparison posttest was used for comparing multiple groups, where appropriate. Groups were considered significantly different when $P < 0.05$.

SUPPLEMENTARY MATERIALS

stm.sciencemag.org/cgi/content/full/13/576/eabc0227/DC1
Materials and Methods

Fig. S1. Liver function tests in recipients after autologous or allogeneic HCT in NHP.

Fig. S2. Gating tree for flow cytometric identification and characterization of T cells within different spatiotemporal compartments using SIVS in NHP.

Fig. S3. Phenotypic characteristics of liver intravascular compartment-1 T cells in NHP.

Fig. S4. Compartmentalization of CD4⁺ T cells at steady state and after HCT in NHP.

Fig. S5. Migration of CD4⁺ and CD8⁺ T cells at steady state and after HCT in NHP.

Fig. S6. Phenotypic characterization of compartment-2 and compartment-3 CD8⁺ T cells in NHP.

Fig. S7. Phenotypic characteristics of intestinal CD4⁺ T cells in NHP.

Fig. S8. Transcriptomic identification of intestinal CD8⁺ T cells in NHP.

Fig. S9. Transcriptomic identification of intestinal T_{RM}-high and T_{RM}-low CD8⁺ T cells from large intestine in NHP.

Fig. S10. Immunophenotypic and transcriptomic characteristics of CD8⁺ T cells from the large intestine.

Fig. S11. Threshold testing of T_{RM}-high and T_{RM}-low CD8⁺ T cells.

Table S1. Transplant characteristics.

Table S2. List of antibodies used, flow cytometry panels, and flow-based definitions of lymphocyte populations.

Table S3. scRNA-seq sample information and QC metrics.

Table S4. Differentially expressed genes between donor, host, and HC CD8⁺ T cells with high enrichment scores for the T_{RM} signature.

Table S5. Pathway analysis of differentially expressed genes between donor, host, and HC CD8⁺ T cells with high enrichment scores for the T_{RM} signature.

Table S6. Predicted activated upstream regulators in donor CD8⁺ T cells with high enrichment scores for the T_{RM} signature in comparison with their HC and host counterparts.

Table S7. Differentially expressed genes between donor, host, and HC CD8⁺ T cells with low enrichment scores for the T_{RM} signature.

Table S8. Pathway analysis of differentially expressed genes between donor, host, and HC CD8⁺ T cells with low enrichment scores for the T_{RM} signature.

Table S9. Predicted activated upstream regulators in donor CD8⁺ T cells with low enrichment scores for the T_{RM} signature in comparison with their HC and host counterparts.

Table S10. Differentially expressed genes between donor CD8⁺ T cells with low and high enrichment scores for the T_{RM} signature.

Table S11. Predicted activated upstream regulators in donor CD8⁺ T cells with low enrichment scores compared to cells with high enrichment scores for the T_{RM} signature.

Table S12. Gene signature of donor CD8⁺ T cells with low enrichment scores for the T_{RM} signature, defined as shown in Fig. 5B.

Table S13. Pathway analysis on the gene signature of donor CD8⁺ T cells with low enrichment scores for the T_{RM} signature.

Table S14. Predicted activated upstream regulators based on the gene signature of donor CD8⁺ T cells with low enrichment scores for the T_{RM} signature.

Table S15. Clinical characteristics of patients from the ABA2 clinical trial (NCT01743131), included in the current study.

Table S16. Results of GSEA analysis comparing patients from the ABA2 clinical trial (NCT01743131) with grade 2 to 4 and 3 to 4 aGVHD versus patients with grade 0 to 1 and 0 to 2 aGVHD, respectively.

Table S17. scRNA-seq-derived gene sets used for GSEA analysis.

Data file S1. Primary data.

References (87–91)

[View/request a protocol for this paper from Bio-protocol.](#)

REFERENCES AND NOTES

- D. Masopust, D. Choo, V. Vezys, E. J. Wherry, J. Duraiswamy, R. Akondy, J. Wang, K. A. Casey, D. L. Barber, K. S. Kawamura, K. A. Fraser, R. J. Webby, V. Brinkmann, E. C. Butcher, K. A. Newell, R. Ahmed, Dynamic T cell migration program provides resident memory within intestinal epithelium. *J. Exp. Med.* **207**, 553–564 (2010).
- M. L. McCully, A. Kozeli, B. Moser, Peripheral tissue chemokines: Homeostatic control of immune surveillance T cells. *Trends Immunol.* **39**, 734–747 (2018).
- S. Zundler, E. Becker, M. Spocinska, M. Slawik, L. Parga-Vidal, R. Stark, M. Wiendl, R. Atreya, T. Rath, M. Leppkes, K. Hildner, R. López-Posadas, S. Lukassen, A. B. Ekici, C. Neufert, I. Atreya, K. van Gisbergen, M. F. Neurath, Hobit- and Blimp-1-driven CD4⁺ tissue-resident memory T cells control chronic intestinal inflammation. *Nat. Immunol.* **20**, 288–300 (2019).
- C. O. Park, T. S. Kupper, The emerging role of resident memory T cells in protective immunity and inflammatory disease. *Nat. Med.* **21**, 688–697 (2015).
- M. E. Snyder, M. O. Finlayson, T. J. Connors, P. Dogra, T. Senda, E. Bush, D. Carpenter, C. Marboe, L. Benvenuto, L. Shah, H. Robbins, J. L. Hook, M. Sykes, F. D'Ovidio, M. Bacchetta, J. R. Sonett, D. J. Lederer, S. Arcasoy, P. A. Sims, D. L. Farber, Generation and persistence of human tissue-resident memory T cells in lung transplantation. *Sci. Immunol.* **4**, eaav5581 (2019).
- J. Zuber, B. Shonts, S. P. Lau, A. Obradovic, J. Fu, S. Yang, M. Lambert, S. Coley, J. Weiner, J. Thome, S. DeWolf, D. L. Farber, Y. Shen, S. Caillat-Zucman, G. Bhagat, A. Griesemer, M. Martinez, T. Kato, M. Sykes, Bidirectional intra-graft alloreactivity drives the repopulation of human intestinal allografts and correlates with clinical outcome. *Sci. Immunol.* **1**, eaah3732 (2016).
- D. Amsen, K. P. J. van Gisbergen, P. Hombrink, R. A. W. van Lier, Tissue-resident memory T cells at the center of immunity to solid tumors. *Nat. Immunol.* **19**, 538–546 (2018).
- S. L. Park, T. Gebhardt, L. K. Mackay, Tissue-resident memory T cells in cancer immunosurveillance. *Trends Immunol.* **40**, 735–747 (2019).
- R. Zeiser, G. Socié, B. R. Blazar, Pathogenesis of acute graft-versus-host disease: From intestinal microbiota alterations to donor T cell activation. *Br. J. Haematol.* **175**, 191–207 (2016).
- B. E. Anderson, P. A. Taylor, J. M. McNiff, D. Jain, A. J. Demetris, A. Panoskaltis-Mortari, A. Ager, B. R. Blazar, W. D. Shlomchik, M. J. Shlomchik, Effects of donor T-cell trafficking and priming site on graft-versus-host disease induction by naive and memory phenotype CD4 T cells. *Blood* **111**, 5242–5251 (2008).
- R. Reshef, S. M. Luger, E. O. Hexner, A. W. Loren, N. V. Frey, S. D. Nasta, S. C. Goldstein, E. A. Stadtmauer, J. Smith, S. Bailey, R. Mick, D. F. Heitjan, S. G. Emerson, J. A. Hoxie, R. H. Vonderheide, D. L. Porter, Blockade of lymphocyte chemotaxis in visceral graft-versus-host disease. *N. Engl. J. Med.* **367**, 135–145 (2012).
- C. A. Wysocki, A. Panoskaltis-Mortari, B. R. Blazar, J. S. Serody, Leukocyte migration and graft-versus-host disease. *Blood* **105**, 4191–4199 (2005).
- A. Beilhack, S. Schulz, J. Baker, G. F. Beilhack, C. B. Wieland, E. I. Herman, E. M. Baker, Y. A. Cao, C. H. Contag, R. S. Negrin, In vivo analyses of early events in acute graft-versus-host disease reveal sequential infiltration of T-cell subsets. *Blood* **106**, 1113–1122 (2005).
- R. El-Asady, R. Yuan, K. Liu, D. Wang, R. E. Gress, P. J. Lucas, C. B. Drachenberg, G. A. Hadley, TGF- β -dependent CD103 expression by CD8⁺ T cells promotes selective destruction of the host intestinal epithelium during graft-versus-host disease. *J. Exp. Med.* **201**, 1647–1657 (2005).
- E. S. P. Santos, S. Ciré, T. Conlan, L. Jardine, C. Tkacz, I. R. Ferrer, C. Lomas, S. Ward, H. West, S. Dertschnig, S. Blobner, T. K. Means, S. Henderson, D. H. Kaplan, M. Collin, V. Plagnol, C. L. Bennett, R. Chakraverty, Peripheral tissues reprogram CD8⁺ T cells for pathogenicity during graft-versus-host disease. *JCI Insight* **3**, e97011 (2018).
- A. Romagnani, V. Vettore, T. Rezzonico-Jost, S. Hampe, E. Rottoli, W. Nadolni, M. Perotti, M. A. Meier, C. Hermanns, S. Geiger, G. Wennemuth, C. Recordati, M. Matsushita, S. Muehlich, M. Proietti, V. Chubanov, T. Gudermann, F. Grassi, S. Zierler, TRPM7 kinase activity is essential for T cell colonization and alloreactivity in the gut. *Nat. Commun.* **8**, 1917 (2017).
- S. N. Furlan, B. Watkins, V. Tkachev, S. Cooley, A. Panoskaltis-Mortari, K. Betz, M. Brown, D. J. Hunt, J. B. Schell, K. Zeleski, A. Yu, C. R. Giver, E. K. Waller, J. S. Miller, B. R. Blazar, L. S. Kean, Systems analysis uncovers inflammatory Th/Tc17-driven modules during acute GVHD in monkey and human T cells. *Blood* **128**, 2568–2579 (2016).
- S. N. Furlan, B. Watkins, V. Tkachev, R. Flynn, S. Cooley, S. Ramakrishnan, K. Singh, C. Giver, K. Hamby, L. Stempora, A. Garrett, J. Chen, K. M. Betz, C. G. Ziegler, G. K. Tharp, S. E. Bosinger, D. E. Promislow, J. S. Miller, E. K. Waller, B. R. Blazar, L. S. Kean, Transcriptome analysis of GVHD reveals aurora kinase A as a targetable pathway for disease prevention. *Sci. Transl. Med.* **7**, 315ra191 (2015).
- W. P. Miller, S. Srinivasan, A. Panoskaltis-Mortari, K. Singh, S. Sen, K. Hamby, T. Deane, L. Stempora, J. Beus, A. Turner, C. Wheeler, D. C. Anderson, P. Sharma, A. Garcia, E. Strobert, E. Elder, I. Crocker, T. Crenshaw, M. C. Penedo, T. Ward, M. Song, J. Horan, C. P. Larsen, B. R. Blazar, L. S. Kean, GVHD after haploidentical transplantation: A novel, MHC-defined rhesus macaque model identifies CD28⁺ CD8⁺ T cells as a reservoir of breakthrough T-cell proliferation during costimulation blockade and sirolimus-based immunosuppression. *Blood* **116**, 5403–5418 (2010).
- V. Tkachev, S. N. Furlan, B. Watkins, D. J. Hunt, H. B. Zheng, A. Panoskaltis-Mortari, K. Betz, M. Brown, J. B. Schell, K. Zeleski, A. Yu, I. Kirby, S. Cooley, J. S. Miller, B. R. Blazar, D. Casson, P. Bland-Ward, L. S. Kean, Combined OX40L and mTOR blockade controls effector T cell activation while preserving T_{reg} reconstitution after transplant. *Sci. Transl. Med.* **9**, eaan3085 (2017).
- H. P. Gideon, E. L. Potter, V. Tkachev, G. Fabbazzi, A. Chasiakos, C. Petrovas, P. A. Darrah, P. L. Lin, K. E. Foulds, L. S. Kean, J. L. Flynn, M. Roederer, Measurement of leukocyte trafficking kinetics in macaques by serial intravascular staining. *Sci. Transl. Med.* **13**, 10.1126/scitranslmed.abb4582, (2021).
- R. Champlin, W. Ho, J. Gajewski, S. Feig, M. Burnison, G. Holley, P. Greenberg, K. Lee, I. Schmid, J. Giorgi, Selective depletion of CD8⁺ T lymphocytes for prevention of graft-versus-host disease after allogeneic bone marrow transplantation. *Blood* **76**, 418–423 (1990).
- N. C. Schattenfroh, R. A. Hoffman, S. A. McCarthy, R. L. Simmons, Phenotypic analysis of donor cells infiltrating the small intestinal epithelium and spleen during graft-versus-host disease. *Transplantation* **59**, 268–273 (1995).
- D. Fernandez-Ruiz, W. Y. Ng, L. E. Holz, J. Z. Ma, A. Zaid, Y. C. Wong, L. S. Lau, V. Mollard, A. Cozijnsen, N. Collins, J. Li, G. M. Davey, Y. Kato, S. Devi, R. Skandari, M. Pauley, J. H. Manton, D. I. Godfrey, A. Braun, S. S. Tay, P. S. Tan, D. G. Bowen, F. Koch-Nolte, B. Rissiek, F. R. Carbone, B. S. Crabb, M. Lahoud, I. A. Cockburn, S. N. Mueller, P. Bertolino, G. I. McFadden, I. Caminschi, W. R. Heath, Liver-resident memory CD8⁺ T cells form a front-line defense against Malaria liver-stage infection. *Immunity* **45**, 889–902 (2016).
- H. A. McNamara, Y. Cai, M. V. Wagle, Y. Sontani, C. M. Roots, L. A. Miosge, J. H. O'Connor, H. J. Sutton, V. V. Ganusov, W. R. Heath, P. Bertolino, C. G. Goodnow, I. A. Parish, A. Enders, I. A. Cockburn, Up-regulation of LFA-1 allows liver-resident memory T cells to patrol and remain in the hepatic sinusoids. *Sci. Immunol.* **2**, eaaj1996 (2017).
- M. Chopra, M. Biehl, T. Steinfatt, A. Brandl, J. Kums, J. Amich, M. Vaeth, J. Kuen, R. Holtappels, J. Podlech, A. Mottok, S. Kraus, A. L. Jordan-Garrote, C. A. Bauerlein, C. Brede, E. Ribechini, A. Fick, A. Seher, J. Polz, K. J. Ottmüller, J. Baker, H. Nishikii, M. Ritz, K. Mattenheimer, S. Schwinn, T. Winter, V. Schafer, S. Krappmann, H. Einsele, T. D. Muller, M. J. Reddhease, M. B. Lutz, D. N. Mannel, F. Berberich-Siebelt, H. Wajant, A. Beilhack, Exogenous TNFR2 activation protects from acute GVHD via host T reg cell expansion. *J. Exp. Med.* **213**, 1881–1900 (2016).
- N. Komatsu, S. Hori, Full restoration of peripheral Foxp3⁺ regulatory T cell pool by radioresistant host cells in *scurfy* bone marrow chimeras. *Proc. Natl. Acad. Sci. U.S.A.* **104**, 8959–8964 (2007).
- A. Arina, M. Beckett, C. Fernandez, W. Zheng, S. Pitroda, S. J. Chmura, J. J. Luke, M. Forde, Y. Hou, B. Burnette, H. Mauceri, I. Lowy, T. Sims, N. Khodarev, Y.-X. Fu, R. W. Weichselbaum, Tumor-reprogrammed resident T cells resist radiation to control tumors. *Nat. Commun.* **10**, 3959 (2019).
- L. K. Mackay, A. Rahimpour, J. Z. Ma, N. Collins, A. T. Stock, M. L. Hafon, J. Vega-Ramos, P. Lauzurica, S. N. Mueller, T. Stefanovic, D. C. Tscharke, W. R. Heath, M. Inouye, F. R. Carbone, T. Gebhardt, The developmental pathway for CD103⁺CD8⁺ tissue-resident memory T cells of skin. *Nat. Immunol.* **14**, 1294–1301 (2013).
- L. K. Beura, N. J. Fares-Frederickson, E. M. Steinert, M. C. Scott, E. A. Thompson, K. A. Fraser, J. M. Schenkel, V. Vezys, D. Masopust, CD4⁺ resident memory T cells dominate immunosurveillance and orchestrate local recall responses. *J. Exp. Med.* **216**, 1214–1229 (2019).
- T. Bergsbaken, M. J. Bevan, Proinflammatory microenvironments within the intestine regulate the differentiation of tissue-resident CD8⁺ T cells responding to infection. *Nat. Immunol.* **16**, 406–414 (2015).
- K. A. Casey, K. A. Fraser, J. M. Schenkel, A. Moran, M. C. Abt, L. K. Beura, P. J. Lucas, D. Artis, E. J. Wherry, K. Hogquist, V. Vezys, D. Masopust, Antigen-independent differentiation and maintenance of effector-like resident memory T cells in tissues. *J. Immunol.* **188**, 4866–4875 (2012).
- N. Zhang, M. J. Bevan, Transforming growth factor- β signaling controls the formation and maintenance of gut-resident memory T cells by regulating migration and retention. *Immunity* **39**, 687–696 (2013).
- R. Bartolome-Casado, O. J. B. Landsverk, S. K. Chauhan, L. Richter, D. Phung, V. Greiff, L. F. Rines, Y. Yao, R. S. Neumann, S. Yaqub, O. Oyen, R. Horneland, E. M. Aandahl, V. Paulsen, L. M. Sollid, S. W. Qiao, E. S. Baekkevold, F. L. Jahnsen, Resident memory CD8 T cells persist for years in human small intestine. *J. Exp. Med.* **216**, 2412–2426 (2019).
- S. Zhou, H. Ueta, X. D. Xu, C. Shi, K. Matsuno, Predominant donor CD103⁺CD8⁺ T cell infiltration into the gut epithelium during acute GVHD: A role of gut lymph nodes. *Int. Immunol.* **20**, 385–394 (2008).
- J. A. Hill, M. Feuerer, K. Tash, S. Haxhinasto, J. Perez, R. Melamed, D. Mathis, C. Benoist, Foxp3 transcription-factor-dependent and -independent regulation of the regulatory T cell transcriptional signature. *Immunity* **27**, 786–800 (2007).

37. J. J. Milner, C. Toma, B. Yu, K. Zhang, K. Omilusik, A. T. Phan, D. Wang, A. J. Getzler, T. Nguyen, S. Crotty, W. Wang, M. E. Pipkin, A. W. Goldrath, Runx3 programs CD8⁺ T cell residency in non-lymphoid tissues and tumours. *Nature* **552**, 253–257 (2017).
38. L. Zhang, X. Yu, L. Zheng, Y. Zhang, Y. Li, Q. Fang, R. Gao, B. Kang, Q. Zhang, J. Y. Huang, H. Konno, X. Guo, Y. Ye, S. Gao, S. Wang, X. Hu, X. Ren, Z. Shen, W. Ouyang, Z. Zhang, Lineage tracking reveals dynamic relationships of T cells in colorectal cancer. *Nature* **564**, 268–272 (2018).
39. B. V. Kumar, W. Ma, M. Miron, T. Granot, R. S. Guyer, D. J. Carpenter, T. Senda, X. Sun, S. H. Ho, H. Lerner, A. L. Friedman, Y. Shen, D. L. Farber, Human tissue-resident memory T cells are defined by core transcriptional and functional signatures in lymphoid and mucosal sites. *Cell Rep.* **20**, 2921–2934 (2017).
40. F. M. Behr, A. Chuwonpad, R. Stark, K. van Gisbergen, Armed and ready: Transcriptional regulation of tissue-resident memory CD8⁺ T cells. *Front. Immunol.* **9**, 1770 (2018).
41. H. Borges da Silva, L. K. Beura, H. Wang, E. A. Hanse, R. Gore, M. C. Scott, D. A. Walsh, K. E. Block, R. Fonseca, Y. Yan, K. L. Hippen, B. R. Blazar, D. Masopust, A. Kelekar, L. Vulchanova, K. A. Hogquist, S. C. Jameson, The purinergic receptor P2RX7 directs metabolic fitness of long-lived memory CD8⁺ T cells. *Nature* **559**, 264–268 (2018).
42. C. Li, B. Zhu, Y. M. Son, Z. Wang, L. Jiang, M. Xiang, Z. Ye, K. E. Beckermann, Y. Wu, J. W. Jenkins, P. J. Siska, B. G. Vincent, Y. S. Prakash, T. Peikert, B. T. Edelson, R. Taneja, M. H. Kaplan, J. C. Rathmell, H. Dong, T. Hitosugi, J. Sun, The transcription factor bhlhe40 programs mitochondrial regulation of resident CD8⁺ T cell fitness and functionality. *Immunity* **51**, 491–507.e7 (2019).
43. Y. Pan, T. Tian, C. O. Park, S. Y. Lofftus, S. Mei, X. Liu, C. Luo, J. T. O'Malley, A. Gehad, J. E. Teague, S. J. Divito, R. Fuhlbrigge, P. Puigserver, J. G. Krueger, G. S. Hotamisligil, R. A. Clark, T. S. Kupper, Survival of tissue-resident memory T cells requires exogenous lipid uptake and metabolism. *Nature* **543**, 252–256 (2017).
44. C. A. Byersdorfer, V. Tkachev, A. W. Opipari, S. Goodell, J. Swanson, S. Sandquist, G. D. Glick, J. L. Ferrara, Effector T cells require fatty acid metabolism during murine graft-versus-host disease. *Blood* **122**, 3230–3237 (2013).
45. E. Gatzka, D. R. Wahl, A. W. Opipari, T. B. Sundberg, P. Reddy, C. Liu, G. D. Glick, J. L. Ferrara, Manipulating the bioenergetics of alloreactive T cells causes their selective apoptosis and arrests graft-versus-host disease. *Sci. Transl. Med.* **3**, 67ra68 (2011).
46. V. M. Hubbard, J. M. Eng, T. Ramirez-Montagut, K. H. Tjoe, S. J. Muriglian, A. A. Kochman, T. H. Terwey, L. M. Willis, R. Schiro, G. F. Heller, G. F. Murphy, C. Liu, O. Alpdogan, M. R. van den Brink, Absence of inducible costimulator on alloreactive T cells reduces graft versus host disease and induces Th2 deviation. *Blood* **106**, 3285–3292 (2005).
47. P. A. Taylor, A. Panoskaltis-Mortari, G. J. Freeman, A. H. Sharpe, R. J. Noelle, A. Y. Rudensky, T. W. Mak, J. S. Serody, B. R. Blazar, Targeting of inducible costimulator (ICOS) expressed on alloreactive T cells down-regulates graft-versus-host disease (GVHD) and facilitates engraftment of allogeneic bone marrow (BM). *Blood* **105**, 3372–3380 (2005).
48. J. Koreth, K.-i. Matsuoka, H. T. Kim, S. M. McDonough, B. Bindra, E. P. Alyea III, P. Armand, C. Cutler, V. T. Ho, N. S. Treister, D. C. Bienfang, S. Prasad, D. Tzachanis, R. M. Joyce, D. E. Avigan, J. H. Antin, J. Ritz, R. J. Soiffer, Interleukin-2 and regulatory T cells in graft-versus-host disease. *N. Engl. J. Med.* **365**, 2055–2066 (2011).
49. L. Perol, G. H. Martin, S. Maury, J. L. Cohen, E. Piaggio, Potential limitations of IL-2 administration for the treatment of experimental acute graft-versus-host disease. *Immunol. Lett.* **162**, 173–184 (2014).
50. B. R. Blazar, A. H. Sharpe, A. I. Chen, A. Panoskaltis-Mortari, C. Lees, H. Akiba, H. Yagita, N. Killeen, P. A. Taylor, Ligation of OX40 (CD134) regulates graft-versus-host disease (GVHD) and graft rejection in allogeneic bone marrow transplant recipients. *Blood* **101**, 3741–3748 (2003).
51. W. Du, X. Cao, Cytotoxic pathways in allogeneic hematopoietic cell transplantation. *Front. Immunol.* **9**, 2979 (2018).
52. T. Ichiba, T. Teshima, R. Kuick, D. E. Misek, C. Liu, Y. Takada, Y. Maeda, P. Reddy, D. L. Williams, S. M. Hanash, J. L. Ferrara, Early changes in gene expression profiles of hepatic GVHD uncovered by oligonucleotide microarrays. *Blood* **102**, 763–771 (2003).
53. Y. Tian, M. A. Cox, S. M. Kahan, J. T. Ingram, R. K. Bakshi, A. J. Zajac, A context-dependent role for IL-21 in modulating the differentiation, distribution, and abundance of effector and memory CD8⁺ T cell subsets. *J. Immunol.* **196**, 2153–2166 (2016).
54. A. M. Hanash, L. W. Kappel, N. L. Yim, R. A. Nejat, G. L. Goldberg, O. M. Smith, U. K. Rao, L. Dykstra, I. K. Na, A. M. Holland, J. A. Dudakov, C. Liu, G. F. Murphy, W. J. Leonard, G. Heller, M. R. van den Brink, Abrogation of donor T-cell IL-21 signaling leads to tissue-specific modulation of immunity and separation of GVHD from GVL. *Blood* **118**, 446–455 (2011).
55. K. L. Hippen, C. Bucher, D. K. Schirm, A. M. Bearl, T. Brender, K. A. Mink, K. S. Waggle, R. Peffault de Latour, A. Janin, J. M. Curtsinger, S. R. Dillon, J. S. Miller, G. Socie, B. R. Blazar, Blocking IL-21 signaling ameliorates xenogeneic GVHD induced by human lymphocytes. *Blood* **119**, 619–628 (2012).
56. B. W. Blaser, S. Roychowdhury, D. J. Kim, N. R. Schwind, D. Bhatt, W. Yuan, D. F. Kusewitt, A. K. Ferketich, M. A. Caligiuri, M. Guimond, Donor-derived IL-15 is critical for acute allogeneic graft-versus-host disease. *Blood* **105**, 894–901 (2005).
57. S. Roychowdhury, B. W. Blaser, A. G. Freud, K. Katz, D. Bhatt, A. K. Ferketich, V. Bergdall, D. Kusewitt, R. A. Baiocchi, M. A. Caligiuri, IL-15 but not IL-2 rapidly induces lethal xenogeneic graft-versus-host disease. *Blood* **106**, 2433–2435 (2005).
58. C. Bucher, L. Koch, C. Vogtenhuber, E. Goren, M. Munger, A. Panoskaltis-Mortari, P. Sivakumar, B. R. Blazar, IL-21 blockade reduces graft-versus-host disease mortality by supporting inducible T regulatory cell generation. *Blood* **114**, 5375–5384 (2009).
59. G. R. Brown, E. L. Lee, D. L. Thiele, TNF enhances CD4⁺ T cell alloproliferation, IFN- γ responses, and intestinal graft-versus-host disease by IL-12-independent mechanisms. *J. Immunol.* **170**, 5082–5088 (2003).
60. F. Masson, M. Ghisi, J. R. Groom, A. Kallies, C. Seillet, R. W. Johnstone, S. L. Nutt, G. T. Belz, Id2 represses E2A-mediated activation of IL-10 expression in T cells. *Blood* **123**, 3420–3428 (2014).
61. S. Takashima, M. L. Martin, S. A. Jansen, Y. Fu, J. Bos, D. Chandra, M. H. O'Connor, A. M. Mertelsmann, P. Vinci, J. Kuttigara, S. M. Devlin, S. Middendorp, M. Calafiore, A. Egorova, M. Kleppe, Y. Lo, N. F. Shroyer, E. H. Cheng, R. L. Levine, C. Liu, R. Kolesnick, C. A. Lindemans, A. M. Hanash, T cell-derived interferon- γ programs stem cell death in immune-mediated intestinal damage. *Sci. Immunol.* **4**, eaay8556 (2019).
62. D. L. Gibbons, L. Abeler-Dorner, T. Raine, I. Y. Hwang, A. Jandke, M. Wencker, L. Deban, C. E. Rudd, P. M. Irving, J. H. Kehrl, A. C. Hayday, Cutting Edge: Regulator of G protein signaling-1 selectively regulates gut T cell trafficking and colitic potential. *J. Immunol.* **187**, 2067–2071 (2011).
63. M. G. Castor, B. Rezende, C. B. Resende, A. L. Alessandri, C. T. Fagundes, L. P. Sousa, R. M. Arantes, D. G. Souza, T. A. Silva, A. E. Proudfoot, M. M. Teixeira, V. Pinho, The CCL3/ macrophage inflammatory protein-1 α -binding protein evasin-1 protects from graft-versus-host disease but does not modify graft-versus-leukemia in mice. *J. Immunol.* **184**, 2646–2654 (2010).
64. O. M. Howard, J. A. Turpin, R. Goldman, W. S. Modi, Functional redundancy of the human CCL4 and CCL4L1 chemokine genes. *Biochem. Biophys. Res. Commun.* **320**, 927–931 (2004).
65. N. Baschuk, N. Wang, S. V. Watt, H. Halse, C. House, P. I. Bird, R. Strugnell, J. A. Trapani, M. J. Smyth, D. M. Andrews, NK cell intrinsic regulation of MIP-1 α by granzyme M. *Cell Death Dis.* **5**, e1115 (2014).
66. J. Bernhagen, R. Krohn, H. Lue, J. L. Gregory, A. Zerneck, R. R. Koenen, M. Dewor, I. Georgiev, A. Schober, L. Leng, T. Kooistra, G. Fingerle-Rowson, P. Ghezzi, R. Kleemann, S. R. McColl, R. Bucala, M. J. Hickey, C. Weber, MIF is a noncognate ligand of CXC chemokine receptors in inflammatory and atherogenic cell recruitment. *Nat. Med.* **13**, 587–596 (2007).
67. C. C. Brinkman, D. Iwami, M. K. Hritz, Y. Xiong, S. Ahmad, T. Simon, K. L. Hippen, B. R. Blazar, J. S. Bromberg, Treg engage lymphotoxin beta receptor for afferent lymphatic transendothelial migration. *Nat. Commun.* **7**, 12021 (2016).
68. Y. Liang, C. Liu, J. Y. Djeu, B. Zhong, T. Peters, K. Scharffetter-Kochanek, C. Anasetti, X. Z. Yu, Beta2 integrins separate graft-versus-host disease and graft-versus-leukemia effects. *Blood* **111**, 954–962 (2008).
69. L. Dupre, R. Houmadi, C. Tang, J. Rey-Barroso, T Lymphocyte Migration: An action movie starring the actin and associated actors. *Front. Immunol.* **6**, 586 (2015).
70. S. Ono, The role of cyclase-associated protein in regulating actin filament dynamics - more than a monomer-sequestration factor. *J. Cell Sci.* **126**, 3249–3258 (2013).
71. J. Kim, M. J. Shapiro, A. O. Bamidele, P. Gurel, P. Thapa, H. N. Higgs, K. E. Hedin, V. S. Shapiro, D. D. Billadeau, Coactosin-like 1 antagonizes cofilin to promote lamellipodial protrusion at the immune synapse. *PLOS ONE* **9**, e85090 (2014).
72. S. D. Desai, R. E. Reed, J. Burks, L. M. Wood, A. K. Pullikuth, A. L. Haas, L. F. Liu, J. W. Breslin, S. Meiners, S. Sankar, ISG15 disrupts cytoskeletal architecture and promotes motility in human breast cancer cells. *Exp. Biol. Med.* **237**, 38–49 (2012).
73. S. H. Hwang, S. H. Jung, S. Lee, S. Choi, S. A. Yoo, J. H. Park, D. Hwang, S. C. Shim, L. Sabbagh, K. J. Kim, S. H. Park, C. S. Cho, B. S. Kim, L. Leng, R. R. Montgomery, R. Bucala, Y. J. Chung, W. U. Kim, Leukocyte-specific protein 1 regulates T-cell migration in rheumatoid arthritis. *Proc. Natl. Acad. Sci. U.S.A.* **112**, E6535–E6543 (2015).
74. R. Schoppmeyer, R. Zhao, H. Cheng, M. Hamed, C. Liu, X. Zhou, E. C. Schwarz, Y. Zhou, A. Knorck, G. Schwarz, S. Ji, L. Liu, J. Long, V. Helms, M. Hoth, X. Yu, B. Qu, Human profilin 1 is a negative regulator of CTL mediated cell-killing and migration. *Eur. J. Immunol.* **47**, 1562–1572 (2017).
75. K. G. Anderson, H. Sung, C. N. Skon, L. Lefrancois, A. Deisinger, V. Vezys, D. Masopust, Cutting edge: Intravascular staining redefines lung CD8⁺ T cell responses. *J. Immunol.* **189**, 2702–2706 (2012).
76. L. K. Mackay, E. Wynne-Jones, D. Freestone, D. G. Pellicci, L. A. Mielke, D. M. Newman, A. Braun, F. Masson, A. Kallies, G. T. Belz, F. R. Carbone, T-box transcription factors combine with the cytokines TGF- β and IL-15 to control tissue-resident memory T cell fate. *Immunity* **43**, 1101–1111 (2015).
77. R. A. Clark, R. Watanabe, J. E. Teague, C. Schlapbach, M. C. Tawa, N. Adams, A. A. Dorosario, K. S. Chaney, C. S. Cutler, N. R. Leboeuf, J. B. Carter, D. C. Fisher, T. S. Kupper, Skin effector memory T cells do not recirculate and provide immune protection in alemtuzumab-treated CTLCL patients. *Sci. Transl. Med.* **4**, 117ra117 (2012).

78. J. M. Schenkel, K. A. Fraser, V. Vezys, D. Masopust, Sensing and alarm function of resident memory CD8⁺ T cells. *Nat. Immunol.* **14**, 509–513 (2013).
79. L. S. Kean, L. A. Turka, B. R. Blazar, Advances in targeting co-inhibitory and co-stimulatory pathways in transplantation settings: The Yin to the Yang of cancer immunotherapy. *Immunol. Rev.* **276**, 192–212 (2017).
80. J. M. Magenau, P. Reddy, Proteasome: Target for acute and chronic GVHD? *Blood* **124**, 1551–1552 (2014).
81. K. L. Hippen, E. G. Aguilar, S. Y. Rhee, S. Bolivar-Wagers, B. R. Blazar, Distinct regulatory and effector T cell metabolic demands during graft-versus-host disease. *Trends Immunol.* **41**, 77–91 (2020).
82. L. K. Beura, P. C. Rosato, D. Masopust, Implications of resident memory T cells for transplantation. *Am. J. Transplant.* **17**, 1167–1175 (2017).
83. A. M. Bolger, M. Lohse, B. Usadel, Trimmomatic: A flexible trimmer for Illumina sequence data. *Bioinformatics* **30**, 2114–2120 (2014).
84. N. L. Bray, H. Pimentel, P. Melsted, L. Pachter, Near-optimal probabilistic RNA-seq quantification. *Nat. Biotechnol.* **34**, 525–527 (2016).
85. M. I. Love, W. Huber, S. Anders, Moderated estimation of fold change and dispersion for RNA-seq data with DESeq2. *Genome Biol.* **15**, 550 (2014).
86. G. Yu, L.-G. Wang, Y. Han, Q.-Y. He, clusterProfiler: An R package for comparing biological themes among gene clusters. *OMICS* **16**, 284–287 (2012).
87. B. R. Blazar, P. A. Taylor, R. McElmurry, L. Tian, A. Panoskaltis-Mortari, S. Lam, C. Lees, T. Waldschmidt, D. A. Valleria, Engraftment of severe combined immune deficient mice receiving allogeneic bone marrow via In utero or postnatal transfer. *Blood* **92**, 3949–3959 (1998).
88. D. R. Zerbino, P. Achuthan, W. Akanni, M. R. Amode, D. Barrell, J. Bhai, K. Billis, C. Cummins, A. Gall, C. G. Girón, L. Gil, L. Gordon, L. Haggerty, E. Haskell, T. Hourlier, O. G. Izuogu, S. H. Janacek, T. Juettemann, J. K. To, M. R. Laird, I. Lavidas, Z. Liu, J. E. Loveland, T. Maurel, W. McLaren, B. Moore, J. Mudge, D. N. Murphy, V. Newman, M. Nuhn, D. Ogeh, C. K. Ong, A. Parker, M. Patricio, H. S. Riat, H. Schuilenburg, D. Sheppard, H. Sparrow, K. Taylor, A. Thormann, A. Vullo, B. Walts, A. Zadissa, A. Frankish, S. E. Hunt, M. Kostadima, N. Langridge, F. J. Martin, M. Muffato, E. Perry, M. Ruffier, D. M. Staines, S. J. Trevanion, B. L. Aken, F. Cunningham, A. Yates, P. Flicek, Ensembl 2018. *Nucleic Acids Res.* **46**, D754–D761 (2018).
89. M. D. Luecken, F. J. Theis, Current best practices in single-cell RNA-seq analysis: A tutorial. *Mol. Syst. Biol.* **15**, e8746 (2019).
90. D. DeTomaso, M. G. Jones, M. Subramaniam, T. Ashuach, C. J. Ye, N. Yosef, Functional interpretation of single cell similarity maps. *Nat. Commun.* **10**, 4376 (2019).
91. G. Korotkevich, V. Sukhov, A. Sergushichev, Fast gene set enrichment analysis. bioRxiv 060012 [Preprint]. 22 October 2019. <https://doi.org/10.1101/060012>.
- Match Foundation Amy Strelzer Manasevit Research Program to V.T.; NIH K23HL136900 to B.W.; NIH R01 HL56067 and NIH R37 AI34495 to B.R.B.; Sloan Fellowship in Chemistry and NIH 2R01 HL095791 to A.K.S.; and Richard and Susan Smith Family Foundation, the HHMI Damon Runyon Cancer Research Foundation Fellowship (DRG-2274-16), the AGA Research Foundation's AGA-Takeda Pharmaceuticals Research Scholar Award in IBD—AGA2020-13-01, the HDDC Pilot and Feasibility P30 DK034854, and the Food Allergy Science Initiative to J.O.-M. **Author contributions:** Conceptualization: V.T., M.R., and L.S.K.; immunological experimentation and data acquisition: V.T., S.N.F., D.J.H., C.M., H.Z., L.C., J.C., and U.G.; immunological data analysis: V.T. and E.L.P.; computational analysis: J.K., J.O.-M., and A.K.S.; development of methodology and providing critical reagents: E.L.P. and M.R.; animal handling and experimentations: M.H., J.O., C.E., and A.B.; histopathological analysis: A.B. and A.P.-M.; human studies: B.W., M.Q., A.L., J.T.H., B.B., K.B., Y.S., B.R.B., and L.S.K.; project administrations: V.T., A.Y., M.H., and L.S.K.; supervision: M.R. and L.S.K.; funding acquisition: V.T., J.O.-M., A.K.S., B.R.B., and L.S.K.; writing—original draft: V.T. and L.S.K.; writing—review and editing: all authors. **Competing interests:** B.W., M.Q., and A.L. report personal fees from Bristol Myers Squibb. J.T.H. reports research funding and personal fees from Bristol Myers Squibb. J.O.-M. reports compensation for consulting services with Cellarity. B.R.B. serves as an advisor to Kamon Pharmaceuticals Inc., Five Prime Therapeutics Inc., Regeneron Pharmaceuticals, Magenta Therapeutics, and BlueRock Therapeutics; he reports research support from Fate Therapeutics, RXi Pharmaceuticals, Alpine Immune Sciences Inc., Abbvie Inc., Leukemia and Lymphoma Society, Children's Cancer Research Fund, and KidsFirst Fund and is a cofounder of Tmunity. A.K.S. reports compensation for consulting and/or scientific advisory board membership from Merck, Honeycomb Biotechnologies, Cellarity, Repertoire Immune Medicines, Ochre Bio, and Dahlia Biosciences. L.S.K. is on the scientific advisory board for HiFiBio; she reports research funding from Kymab Limited, Magenta Therapeutics, BlueBird Bio, and Regeneron Pharmaceuticals. She reports consulting fees from Equillium, Vertex, Novartis Inc., EMD Serono, Gilead Sciences, Interrius, Takeda Pharmaceuticals, and Bristol Myers Squibb. The other authors declare no competing interests. **Data and materials availability:** All data associated with this study are present in the paper or the Supplementary Materials. The NHP scRNA-seq data were deposited in the NCBI's Gene Expression Omnibus database (GSE142483). The RNA-seq data from the ABA2 clinical trial were deposited in the NCBI's Gene Expression Omnibus database (GEO157280).

Submitted 8 April 2020

Accepted 11 December 2020

Published 13 January 2021

10.1126/scitranslmed.abc0227

Citation: V. Tkachev, J. Kaminski, E. L. Potter, S. N. Furlan, A. Yu, D. J. Hunt, C. McGuckin, H. Zheng, L. Colonna, U. Gerdemann, J. Carlson, M. Hoffman, J. Olvera, C. English, A. Baldessari, A. Panoskaltis-Mortari, B. Watkins, M. Qayed, Y. Suessmuth, K. Betz, B. Bratrude, A. Langston, J. T. Horan, J. Ordovas-Montanes, A. K. Shalek, B. R. Blazar, M. Roederer, L. S. Kean, Spatiotemporal single-cell profiling reveals that invasive and tissue-resident memory donor CD8⁺ T cells drive gastrointestinal acute graft-versus-host disease. *Sci. Transl. Med.* **13**, eabc0227 (2021).

Acknowledgments: We thank the veterinary and animal husbandry staff at the Washington National Primate Research Center and H. Leung at the Boston Children's Hospital/Harvard Medical School Microscopy Core. Figures 1F, 3H and 5E were created using BioRender.com. **Funding:** This project was funded by the following grants: NIH 2U19 AI051731, NIH 2R01 HL095791, NIH/FDA, R01 FD004099, and CURE Childhood (<https://curechildhoodcancer.org>) to L.S.K.; ASTCT New Investigator Award and CIMBTR/Be the

Spatiotemporal single-cell profiling reveals that invasive and tissue-resident memory donor CD8 T cells drive gastrointestinal acute graft-versus-host disease

Victor Tkachev James Kaminski E. Lake Potter Scott N. Furlan Alison Yu Daniel J. Hunt Connor McGuckin Hengqi Zheng Lucrezia Colonna Ulrike Gerdemann Judith Carlson Michelle Hoffman Joe Olvera Chris English Audrey Baldessari Angela Panoskaltsis-Mortari Benjamin Watkins Muna Qayed Yvonne Suessmuth Kayla Betz Brandi Bratrude Amelia Langston John T. Horan Jose Ordovas-Montanes Alex K. Shalek Bruce R. Blazar Mario Roederer Leslie S. Kean

Sci. Transl. Med., 13 (576), eabc0227. • DOI: 10.1126/scitranslmed.abc0227

SIVS ing through GVHD

Currently, there are few ways to track leukocyte movements in vivo. Potter and colleagues developed a method to track leukocyte migration in vivo called serial intravascular staining or SIVS. The authors infused differently labeled antibodies at different time points to reveal distinct leukocyte population kinetics in healthy macaques and those infected with *Mycobacterium tuberculosis*. Tkachev *et al.* then applied SIVS to shed light on donor T cell trafficking in macaques that developed acute graft-versus-host disease (GVHD) after transplant. They found that donor cytotoxic CD8 T cells infiltrated the gastrointestinal tract and developed the transcriptional signature of tissue-resident memory T cells. SIVS will be useful for revealing leukocyte trafficking kinetics not only in GVHD and infection but in a variety of other diseases as well.

View the article online

<https://www.science.org/doi/10.1126/scitranslmed.abc0227>

Permissions

<https://www.science.org/help/reprints-and-permissions>

Use of this article is subject to the [Terms of service](#)

Science Translational Medicine (ISSN 1946-6242) is published by the American Association for the Advancement of Science, 1200 New York Avenue NW, Washington, DC 20005. The title *Science Translational Medicine* is a registered trademark of AAAS. Copyright © 2021 The Authors, some rights reserved; exclusive licensee American Association for the Advancement of Science. No claim to original U.S. Government Works